Determination of Atmospheric Lifetimes via the Measurement of OH Radical Kinetics

Michael J. Kurylo* and Vladimir L. Orkin*

Physical and Chemical Properties Division, National Institute of Standards and Technology, Gaithersburg, Maryland 20899

Received April 18, 2003

Contents

1. Introduction

The chemical composition of the earth's atmosphere has been an area of general research interest for many decades.[1] However, increased attention to a number of environmental issues has fostered a more detailed focus in recent years. These environmental drivers include such topics as (i) the destruction of stratospheric ozone via photochemical cycles involving industrial halocarbons and their reaction products,[2] (ii) the alteration of the radiative balance of the earth's atmosphere due to the buildup of infrared absorbing gases and other constituents in the upper troposphere and lower stratosphere,[3] (iii) the production and transport of ozone and other pollutants in the troposphere,[4−8] and (iv) the role of the atmospheric sulfur cycle in aerosol and cloud particle formation.[9,10] Each topic requires quantitative information on the mechanistic details and time scales for atmospheric chemical transformations. Inherent in such quantification are the atmospheric lifetimes of the applicable source gases and the rates of the initial (generally oxidative) steps in their atmospheric degradation. In this paper, we will examine the concept of an atmospheric lifetime, the role that reactions of tropospheric hydroxyl radicals (OH) play in its quantification, the range of methods used for its estimation, and its applicability in quantifying some environmental impacts of source gas emissions. We will then review the various laboratory techniques used in the experimental determination of OH rate constants, and after examining some of the possible errors associated with each, we will discuss some of the difficulties encountered in producing a recommended data set for atmospheric modeling purposes.

* Address correspondence to either author. E-mail: michael.kurylo@nist.gov (M.J.K.); vladimir.orkin@nist.gov (V.L.O.).

2. Atmospheric Burden and Lifetime

2.1. Conceptual Framework

The definition and quantification of an atmospheric residence time or lifetime for a trace gas emitted at the earth's surface are fundamental to understanding the relationship between the budget and the trends of that gas and one or more of the environmental issues mentioned in the introduction. When properly balanced, the budget of a trace gas, RH, will quantitatively account for the various sources and sinks of the gas together with its global atmospheric burden or concentration (C_{RH}^{global}). The latter is defined as the total mass of the gas integrated over the entire atmosphere (troposphere and stratosphere), although the identification of individual burdens for these different regions (C_{RH}^{trop} and C_{RH}^{strat}) can also be important in quantifying certain environmental impacts. These burdens are often defined for modeling purposes as the products of molar or mass mixing

10.1021/cr020524c CCC: $44.00
Published on Web 11/05/2003

Michael J. Kurylo is a chemist at the National Institute of Standards and Technology in Gaithersburg, MD, where he is a member of a research group engaged in gas-phase free radical photochemistry and kinetics with an emphasis on atmospheric processes pertinent to stratospheric ozone depletion and changing atmospheric composition. He also serves on a U.S. Government Inter-Agency detail from NIST to the National Aeronautics and Space Administration Headquarters as manager of NASA's Upper Atmosphere Research Program. Mike received a B.S. in Chemistry from Boston College in 1966 and a Ph.D. in Physical Chemistry from the Catholic University of America in 1969. He subsequently received a National Academy of Sciences National Research Council Postdoctoral Fellowship for research at the National Bureau of Standards (now NIST). He is an author or coauthor of more than 135 scientific publications and has given more than 170 technical presentations nationally and internationally. He has served as a reviewer, contributing author, and lead author for chapters on ozone-related trace gases appearing in the last five international assessments of ozone depletion. He is the recipient of the U.S. Department of Commerce Bronze (1983) and Silver (1991) Medals, the NASA Exceptional Service Medal (1996), the Catholic University of America Alumni Achievement Award in Science (1996), and the NOAA Environmental Hero Award (2000), as well as numerous NASA Group Achievement Awards and United Nations Environment Program Certificates of Recognition. When not immersed in his research and program management activities, Mike, with his wife Mary, focus their attention on their children and growing number of grandchildren (four and counting). As an avid golfer, Mike can occasionally be found on the various links in the Maryland region.

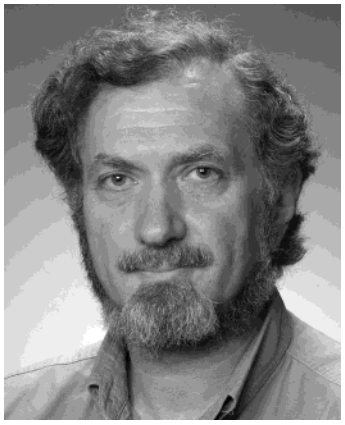

Vladimir L. Orkin is a research chemist at the National Institute of Standards and Technology. He is a member of NASA Panel for Kinetic and Photochemical Data Evaluation. He received his M.S. in 1975 from the Moscow Institute of Physics and Technology (Russia) and his Ph.D. in Chemical Physics from the Institute of Chemical Physics, Russian Academy of Sciences (RAS), Moscow, in 1983. Vladimir joined NIST's Chemical Kinetics and Thermodynamics Division in 1993. During 1997–1999, he worked in the Laboratory of Extraterrestrial Physics at NASA Goddard Space Flight Center (Greenbelt, MD). Since 1987, he headed a research group at the Institute of Energy Problems of Chemical Physics, RAS, for studying photochemical properties of industrial chemicals and estimating their impact on the stratospheric ozone layer to support Russian state program on CFCs and Halons alternatives. His current research interests are gas kinetics, photochemistry and its technical applications, and atmospheric chemistry. Outside of chemical kinetics, Vladimir, a certified professional diver since 1973, is a sailor who loves his family and friendship with his grown-up son, Alik.

ratios in the region of interest (X_{RH}^{trop} and X_{RH}^{strat}) times the total atmospheric mass of that region (M^{trop} and M^{strat})

$$C_{RH}^{trop} = X_{RH}^{trop} M^{trop} \quad (1)$$

$$C_{RH}^{strat} = X_{RH}^{strat} M^{strat} \quad (2)$$

with the global burden being the sum of those in the troposphere and stratosphere.

$$C_{RH}^{global} = C_{RH}^{trop} + C_{RH}^{strat} \quad (3)$$

The global atmospheric lifetime (τ_{RH}^{global}) of a trace gas is the time required to turn over or exchange its global burden.[11] The lifetime depends on both atmospheric chemistry and dynamics and, therefore, may depend on the location of the sources.[12] A trend in the burden occurs when the magnitudes of the sources (emissions or production terms, *P*'s) and sinks (loss terms, *L*'s) differ. For a gas whose atmospheric burden is not changing (i.e., is in steady state), the atmospheric lifetime (defined as the ratio of the global atmospheric burden to the total atmospheric removal rate) can be written as

$$\tau_{RH}^{global} = C_{RH}^{global}/L_{RH}^{global} = X_{RH}^{global} M^{global}/L_{RH}^{global} = C_{RH}^{global}/P_{RH}^{global} \quad (4)$$

where the global losses are the sum of those in the troposphere and stratosphere or in another exchangeable reservoir (e.g., CH_3Br in the ocean mixing layer).[13]

$$L_{RH}^{global} = L_{RH}^{trop} + L_{RH}^{strat} \quad (5)$$

The global lifetime is one of the key factors that determine the environmental impact of a source gas emitted to the atmosphere. Similar equations can be written for any of the subregions into which the atmosphere can be divided for the purpose of modeling.

$$\tau_{RH}^{i} = C_{RH}^{i}/L_{RH}^{i} = X_{RH}^{i} M^{i}/L_{RH}^{i} \quad (6)$$

where *i* denotes the troposphere, stratosphere,[14] or even smaller regions, which have utility in modeling the environmental effects. When defined thusly, the loss rate for a specified region is quantified relative to the burden of the species only within that region (not within the global atmosphere) and the global lifetime is related to the region lifetimes by a mass-weighted sum of reciprocals, that is,

$$(\tau_{RH}^{global})^{-1} = \frac{\sum_i C_{RH}^{i} (\tau_{RH}^{i})^{-1}}{C_{RH}^{global}} \quad (7)$$

However, it is more useful to consider how a loss process in a particular region of the atmosphere affects the global burden of a trace gas. For such purposes, the region lifetimes (τ^i_{RH}) of a species RH can be redefined to reflect their relation to the global atmospheric burden of that species.[15,16]

$$\tau^i_{RH} = C^{global}_{RH}/L^i_{RH} \quad (8)$$

Thus, the mass weighting is no longer necessary and eq 7 can be rewritten as

$$(\tau^{global}_{RH})^{-1} = \sum_i (\tau^i_{RH})^{-1} \quad (9)$$

where τ^i_{RH} are defined by eq 8. This is the definition of loss rates that we will use in this paper, similar to the discussions in an earlier review of this topic.[17]

In the case of uniform distribution of the compound within a particular region, its local loss rate can be presented as

$$L^i_{RH} = \sum_j k^i_j C^i_{RH} \quad (10)$$

where $k_j{}^i$ are first-order rate coefficients associated with various removal processes in the ith region. Thus, combining eqs 8−10, the lifetime of a species in the global atmosphere can be calculated as

$$(\tau^{global}_{RH})^{-1} = \frac{\sum_i \sum_j k^i_j C^i_{RH}}{C^{global}_{RH}} \quad (11)$$

However, given that all species (and their loss processes) are not uniformly distributed over the entire atmosphere, τ^{global}_{RH} should really be calculated by integrating over the atmosphere rather than summing over the regions

$$(\tau^{global}_{RH})^{-1} = \frac{\int_{atmos} \sum_j k_j(V)\, C_{RH}(V)\, dV}{C^{global}_{RH}} = \frac{\sum_j \int_{atmos} k_j(V)\, C_{RH}(V)\, dV}{C^{global}_{RH}} = \sum_j (\tau^j_{RH})^{-1} \quad (12)$$

where τ^j_{RH} is the lifetime of the source gas due to its removal via a particular jth process calculated for the global atmosphere. Note the similarities between eq 12 and eq 9, where the global atmospheric lifetime can be determined as a summation either over atmospheric regions (eq 9) or over atmospheric loss processes (eq 12).

Generally speaking, neither the temporal behavior of the global burden of a source gas nor its concentration in any local region can be described by an exponential dependence with a single decay parameter, τ^{global}_{RH}. Rather, it will have a complicated functional dependence described by parameters associated with inter-region transport rates and local loss rate coefficients, k^i_j. Nevertheless, the global atmospheric lifetime as defined has important utility as a factor for assessing the integrated impact on the earth's atmosphere due to emission of a source gas.

For long-lived source gases, which are well-mixed over the troposphere, eq 11 can be simplified as

$$(\tau^{global}_{RH})^{-1} = \sum_j k^{trop}_j + (\tau^{strat}_{RH})^{-1} = (\tau^{trop}_{RH})^{-1} + (\tau^{strat}_{RH})^{-1} \quad (13)$$

where the j's refer to different tropospheric removal processes. In such cases, the tropospheric lifetime can be calculated from rate constants for removal processes (k_j) and, therefore, the atmospheric lifetime can be determined on the basis of results of laboratory studies of these processes. The term for the stratospheric lifetime cannot be as easily simplified. Because of very slow transport and the very strong altitudinal dependence of incoming UV radiation between about 200 and 220 nm, an absorbing source gas is never distributed uniformly over the entire stratosphere. Therefore, even for a long-lived compound, which is well-mixed in the troposphere, the stratospheric lifetime can only be obtained from detailed modeling of photolysis and transport. Note that for the majority of hydrogen-containing source gases the dominating removal process is their reaction with tropospheric hydroxyl, and $(\tau^{strat}_{RH})^{-1}$ is usually only a small correction in eq 13.

For well-mixed (relatively long-lived) source gases whose burdens change on long time scales, τ^{global}_{RH} does a reasonable job in describing their changing burdens. This is important (and useful) in assessing and evaluating possible environmental impacts due to emission of industrial chemicals. This will be illustrated in a later discussion of time-dependent ozone depletion potentials (ODPs) and global warming potentials (GWPs).

In cases where one or more of the loss processes are not strictly first order in the concentration of the species of interest, the concept of a lifetime is still valid and it can be computed using instantaneous first-order rate coefficients. For some species, the atmospheric lifetime can depend on their own atmospheric abundances; that is, there are chemical feedbacks that can alter the rate of a loss process. Perhaps the best-known example of this is methane (CH_4), whose tropospheric concentration is largely controlled via its reaction with the hydroxyl radical and directly influences the tropospheric OH concentration via the same reaction. Thus, an increase in the atmospheric abundance of CH_4 reduces the OH concentration and leads to a longer CH_4 lifetime.[18−20] A more complex (and opposite) chemical feedback occurs for N_2O. In this case, an increase in the atmospheric abundance of N_2O increases the abundance of NO_x in the stratosphere, thereby depleting stratospheric ozone and increasing the UV flux in the atmosphere. This subsequently leads to more rapid photolysis of N_2O and a shorter lifetime.[23]

2.2. Atmospheric Removal Processes

There is a variety of processes that act to remove a trace gas from either the troposphere or the

stratosphere (or, in some cases, from both). For reactive trace gases (which are the focus of this review), the main tropospheric loss occurs via gas-phase oxidation reactions involving OH (throughout the sunlit troposphere), O_3 and NO_x (during both day and night, especially in polluted urban environments), and Cl (primarily in the boundary layer over oceanic regions). Tropospheric photolysis can become important (depending on the rates of other loss processes) for gases having absorption cross sections $>10^{-23}$ cm^2 at wavelengths greater than about 300 nm. There are several heterogeneous reaction processes that can also be important in the troposphere.[21] These include uptake and hydrolysis in the oceans, uptake and microbial loss in soils and other terrestrial ecosystems, and removal by hydrolysis in clouds or aerosols. Of these three, oceanic removal is generally considered to be the most important, given the sparse data on soil interactions and limited applicability of cloud hydrolysis to more than a few species.[22] Stratospheric loss processes are essentially limited to gas phase reactions [principally with OH and O(^{1}D)] and to UV photolysis. Solar radiation between about 200 and 220 nm penetrating the stratosphere makes photolysis in this region typically a more important atmospheric sink than it is in the troposphere because of generally much larger absorption cross sections of chemicals in this wavelength range (with the exception of I- and multi-Br-containing hydrocarbons that are rapidly photolyzed in the troposphere at wavelengths longer than 300 nm).

In most cases, the lifetime of a relatively long-lived gas does not depend on the geographical location of its emission to the atmosphere and is, therefore, an environmental property of the compound. However, depending on the time scales over which the various loss processes occur, transport from one region of the atmosphere to another can play an important role in the determination of the lifetime/residence time.[13,23−25] For example, the lifetimes of short-lived (i.e., highly reactive) gases are controlled primarily by loss processes near the location of their sources, and transport from such locations is often limited. Thus, these gases are generally not well-mixed throughout an atmospheric region and their concentrations will be largest near the source regions and away from the sink regions. As a result, the lifetimes of such species will depend on the location and season of their emissions and are not unique environmental properties of the compounds in contrast to the long-lived ones. Even for species whose atmospheric lifetimes exceed the approximate $^1/_2$-year time scale required for intra-hemispheric mixing, the lifetime may not be a constant. This can be due either to temporal variations (on short or long time scales) in the reactive species responsible for the loss or to the existence of a highly complex set of control mechanisms and exchanges between different reservoirs. An example of this latter case is CO_2, whose abundance is controlled by exchange among the atmospheric, oceanic, and terrestrial reservoirs via processes occurring on different time scales.[26] Another example of the crucial role of transport is the direct injection of a chemical in the lower stratosphere, for example, emissions from aircraft. As a result of slow transport to the troposphere, the real lifetime will be dictated by reactions and photolysis in the lower stratosphere and can be either longer or shorter than the atmospheric lifetime of the same compound calculated for tropospheric release.

Unless the chemical lifetime of a gas whose emissions occur primarily at the ground is exceptionally short (i.e., shorter than the tropospheric vertical mixing time of 1 or 2 months), trace gas concentrations will exhibit little decrease from the ground up to the tropopause. For gases having lifetimes for tropospheric chemical removal in excess of several years, transport from the troposphere to the stratosphere can play an important role in exposing the gas to loss processes occurring at various altitudes in the stratosphere. Stratospheric photolysis occurs primarily in the region of highest solar flux between about 200 to 220 nm, and differences in UV cross sections for various trace gases result in differences in the altitudes at which the photolysis rate for each gas becomes comparable to its vertical diffusion rate. Thus, the change in atmospheric density with altitude is the principal source of differences in the stratospheric photolysis lifetimes of trace gases.

3. Tropospheric OH

3.1. Atmospheric Sources and Measurements

As discussed in the previous section, the troposphere is a well-mixed system, with intra-hemispheric mixing occurring on a time scale of several months and inter-hemispheric exchange having a time scale of a couple of years. Thus, a small loss process for a trace gas can have a significant effect in removing that gas from the atmosphere even when that process occurs on a local scale. The hydroxyl radical is the most important oxidizing species in the global troposphere.[1,7,8,27] As a result of its role in initiating the majority of oxidation reaction chains, the OH radical is the primary cleansing agent for the lower atmosphere and has been called the "tropospheric vacuum cleaner".[28]

The dominant production cycle for tropospheric OH involves the reaction of O(^{1}D), produced from the photolysis of O_3, with H_2O.

$$O_3 + h\nu \rightarrow O(^1D) + O_2 \qquad \text{(R1)}$$

$$O(^1D) + H_2O \rightarrow OH + OH \qquad \text{(R2)}$$

However, its subsequent reactions with O_3, CO, and CH_4 (and other volatile organic carbon compounds, VOCs) in the presence of nitrogen oxides (NO_x) lead to the formation of HO_2, hydrogen peroxide, alkyl peroxy radicals, and ultimately to the production of ozone via the conversion of NO to NO_2.[7,29] As a result of this complex series of reactions, the tropospheric abundance of OH depends on the abundances of each of these aforementioned species in addition to the tropospheric level of solar UV radiation at wavelengths longer than 300 nm. These dependences result in significant geographic, diurnal, and seasonal variations in the tropospheric OH abundance. Fur-

ther, its dependence on CH_4, CO, and VOCs has led to speculation regarding human influences on its abundance since pre-industrial times. Direct accurate measurement of the OH radical within the atmosphere has proved to be exceptionally challenging, given its low ambient abundance and high temporal and spatial variability. Nevertheless, technological advances in both in situ and remote sensing instrumentation have allowed significant achievements in the measurement area. Both direct (spectroscopic detection of OH) and indirect (chemical conversion followed by direct detection of the new species) approaches have been utilized over more than two decades to determine the OH concentration and its possible trends.[30]

Perhaps the most quantitative success has been achieved for the stratosphere,[31−34] where measurements of OH, HO_2, and several related chemical constituents have demonstrated a high level of understanding of HO_x photochemistry.[35−37] The greater temporal and spatial variability of OH in the troposphere, coupled with the higher ambient pressure and detection interference from other more abundant trace species, has posed additional measurement challenges. While there have been a number of successful achievements using in situ and remote sensing techniques,[38] these have been focused on the high natural variability of OH in response to changing atmospheric composition.[39−42]

3.2. Estimates of the Global Tropospheric OH Distribution

Given that the global distribution of tropospheric OH is much too heterogeneous to be mapped by direct measurements, estimates of the mean global OH concentration have been made using two methods. The first method involves calculating the OH field using chemical transport models (CTMs) validated with observed chemical climatologies.[43−46] Uncertainties in the results of such model calculations arise from uncertainties in the chemistry itself as well as uncertainties in transport, OH precursor abundances, and UV field. The calculation of the atmospheric lifetime of a gas using a CTM involves specifying the global distribution of the gas (or calculating it from an emission scenario) and then integrating the loss of the compound globally.[21]

When the second method is used, the OH field is derived from budget calculations of a proxy gas whose abundance and trends are accurately determined from global measurements and whose sources and sinks are well-quantified.[47−55] It is particularly important that the tropospheric abundance of the proxy gas is essentially controlled by reaction with OH, thereby permitting calculation of the global OH field that reproduces the time series and abundance of the gas. Uncertainties in the results from such proxy calculations derive from uncertainties in the global measurement record and the completeness of knowledge of the sources and sinks of the proxy compound. The use of several commonly used proxies (CH_3CCl_3, CHF_2Cl, CH_2Cl_2, C_2Cl_4, and ^{14}CO) has been reviewed in ref 44c. This study suggests that the cumulative uncertainty in the OH concentration derived from such analyses ranges from 20 to 30%. Differences in the proxy results using different compounds can be attributed in part to differences in the lifetimes of the proxy gases that translate into different regional weightings of the OH concentration. Clearly, the best proxy gases are those for which the previously mentioned uncertainties are minimized and which have sufficiently long atmospheric lifetimes such that they are well-mixed throughout the troposphere. Nevertheless, the use of proxies with shorter lifetimes provides useful information regarding transport (as in the case of ^{14}CO)[53−55] and on local and regional differences in the OH field. Proxy chemicals whose source is primarily industrial (and, hence, focused at northern mid-latitudes) generally exhibit quantifiable Northern Hemisphere/Southern Hemisphere gradients that can be used to constrain both the global and hemispheric mean OH abundances.

3.3. Estimation of the Atmospheric Lifetime Due to Reaction with Tropospheric OH

In both the CTM and proxy methods, accurate rate constants for the reactions of the various trace gases with tropospheric OH are essential input parameters. The OH fields derived from both methods are in reasonable agreement, lending confidence to their use in determining the atmospheric lifetimes of various hydrohalocarbons (the hydrochlorofluorocarbons, HCFCs, and the hydrofluorocarbons, HFCs). While the most robust determination of a trace gas lifetime can be made via CTM calculations as described previously, a simple estimation procedure based on comparison with an appropriate proxy gas can be very useful in assessing a gas' environmental impacts. This procedure is based on the atmospheric lifetime of methyl chloroform (CH_3CCl_3, MCF) determined from a comprehensive analysis of the long-term record of its abundance in the atmosphere coupled with detailed emission inventories and knowledge of its removal mechanisms.[49−51] Using measurements from the entire period (1978−2000) of the ALE/GAGE/AGAGE network[49b,56] together with detailed industrial emissions inventories, Prinn and coworkers[49c] calculated a global average OH concentration of 9.4×10^5 cm^{-3} and a total atmospheric lifetime, τ_{MCF}^{global}, of 4.9 years. When the contributions for stratospheric and oceanic losses are accounted for, these authors derived a CH_3CCl_3 lifetime with respect to removal by tropospheric OH of 5.99 years (τ_{MCF}^{OH}), defined as in eq 8 as the total atmospheric burden of CH_3CCl_3 divided by its rate of destruction by OH in the troposphere. The validity of this determination is based on some rather unique aspects of MCF in the atmosphere. Most importantly, this chemical is almost entirely of industrial origin, and its use as a solvent allows one to essentially equate industrial production figures (for which detailed information is available)[49c] into atmospheric emissions with very little time lag. While possible emissions of CH_3CCl_3 occur from biomass burning, vegetation, and soils, these were considered too small for inclusion in the scenarios used for the previous calculation but were considered in the error analysis. As indicated by eq 8, the lifetime characterizing the

removal by the reaction with OH in the troposphere can be calculated as

$$1/\tau^{OH}_{MCF} = \frac{\int_{trop} k_{MCF}(T)[OH][MCF]\,dV}{\int_{trop+strat}[MCF]\,dV} \quad (14)$$

where $k_{MCF}(T)$ is the rate constant for the reaction between OH and MCF.[57] This inverse lifetime can be approximated as the product of an average tropospheric value for k_{MCF} and an "effective" global tropospheric concentration of OH, $\overline{[OH]}_{global}$

$$1/\tau^{OH}_{MCF} = k_{MCF}(272\ K)\overline{[OH]}_{global} \quad (15)$$

(The selection of $T = 272$ K for calculating an average tropospheric value for $k_{MCF}(T)$ is discussed below.) $\overline{[OH]}_{global}$ has utility in estimating the lifetimes of numerous trace gases. Using eq 15 to calculate $\overline{[OH]}_{global}$, we obtain

$$\overline{[OH]}_{global} = 8.8 \times 10^5\ molecule/cm^3 \quad (16)$$

This value is slightly smaller than the value of the average OH concentration of 9.93×10^5 molecules/cm^3 obtained by Prinn et al.[49c] from model calculations. This difference is due primarily to the temperature dependence of k_{MCF}, which is not accounted for in the model calculations.[49c]

As a result of restrictions on the production of ozone-depleting chemicals, the atmospheric concentration of MCF has been declining for the past 10 years. A recent analysis of flask data from the NOAA/CMDL network[51] for 1992−2000 (a period during which the budget of MCF was controlled primarily by atmospheric removal rather than by industrial production and release) yielded similar results for the global MCF lifetime. Data over this period indicate a diminishing concentration gradient between the two hemispheres (as expected following the cessation of emissions)[44c] and a higher concentration of OH in the tropics of both hemispheres than at higher latitudes. Calculations performed using data records for which the trend is dominated by atmospheric loss processes are less sensitive to uncertainties in the source strengths and, in the limit of zero emissions, become insensitive to calibration accuracy. Hence, it is of interest to examine how long the declining record of MCF abundance will be useful for estimating OH distributions and trends. A recent analysis of this issue by the AGAGE Science Team[58] suggests that the precision and accuracy of existing instrumentation are sufficient to allow the MCF concentration record (under its projected rate of decline) to be useful for these purposes at least through the end of the present decade. There are a number of other industrially produced trace gases whose budget records are under consideration for OH estimation studies. However, current emission uncertainties need to be reduced before such species can be competitive with CH_3CCl_3 for such purposes.[59] Thus, gases that have an appreciable component of their emissions associated with natural sources are of limited use.

As pointed out in an early study,[44b] two species having similar global distributions and having tropospheric removals that are dominated by their reactions with OH will have lifetimes (with respect to OH) that scale inversely by the factor by which their OH rate constants differ. However, the scaling becomes more complex when the rate coefficients have different temperature dependences. For example, species whose reactions with OH have higher activation energies than that for the reaction of OH with MCF will have their removal shifted to warmer temperatures (i.e., in the lower troposphere and in the tropics). In contrast, species having much lower activation energies for their reactions with OH will react very rapidly with OH and their removal rates will be determined by the OH concentration in the atmospheric region of their release.

The authors of ref 44b examined the situation for Arrhenius activation energies ranging from 0 to 2300 K to determine an appropriate scaling temperature for use in determining the ratios of the reaction rates. It was determined that use of a scaling temperature of 277 K resulted in less than 2% errors for activation energies in the range 800−2300 K and less than 7% over the full range of activation energies considered. In a more recent study,[44c] the effect of an updated distribution of tropospheric OH was investigated and a scaling temperature of 272 K was found to be more appropriate (with less than a 5% error over an activation energy range of 0−2500 K). These errors are reduced further if temperatures of 270 and 277 K are used for the lower and higher parts of the range, respectively. When this new scaling temperature is used, the tropospheric lifetime of a species whose atmospheric abundance is controlled primarily by reaction with OH can be calculated relative to that of MCF using the following equation:

$$\tau^{OH}_{RH} = \frac{k_{MCF}(272\ K)}{k_{RH}(272\ K)}\tau^{OH}_{MCF} \quad (17)$$

where τ^{OH}_{RH} and τ^{OH}_{MCF} are the lifetimes of the compound of interest and MCF, respectively, due to reactions with hydroxyl radicals in the troposphere only, and $k_{RH}(272\ K)$ and $k_{MCF}(272\ K) = 6.0 \times 10^{-15}$ cm^3 molecule^{-1} s^{-1} (ref 57) are the rate constants for the reactions of OH with these substances at $T = 272$ K. The value of $\tau^{OH}_{MCF} = 5.99$ years was obtained as described previously[49c] from the measured lifetime of MCF of 4.9 years when an ocean loss of 89 years and a stratospheric loss of 39 years were taken into account using the formulation of eq 9.

It should be emphasized that eq 17 is most applicable for long-lived species that are well-distributed throughout the troposphere. Its use for short-lived gases having lifetimes shorter than the characteristic time of mixing processes in the troposphere can result in significant errors due to the large spatial gradients that were discussed earlier for such chemicals. For such species, eq 17 provides only rough estimates of the tropospheric lifetimes with respect to reaction with OH. The correct residence time of short-lived compounds in the atmosphere will depend on the emission location and season as well as local

atmospheric conditions. The details can be found in some recent atmospheric modeling publications.[60,61] Nevertheless, the results of these modeling studies demonstrate that such an estimation procedure gives reasonable average values and provides a useful scaling of the lifetimes of such compounds.

There are two additional corrections that may be important for lifetimes approximated using eq 17.[62] The first correction is due to possible differences between the stratospheric distributions of MCF (the reference chemical) and the chemical of interest. As a result of its strong absorption of stratospheric UV radiation, MCF is nearly completely photolyzed at altitudes above 22 km[63,64] and, hence, has a nonuniform stratospheric distribution. This can be contrasted to alkanes, fluorinated alkanes (HFCs and some HCFCs), and other compounds that do not absorb in the stratospheric transparency window near 200 nm and, hence, have much smaller stratospheric sinks. Because the actual loss rate in any region of the atmosphere is concentration-dependent, this difference in stratospheric reservoirs can be taken into account using a modified version of eq 17.

$$\tau_{RH}^{OH} = \frac{k_{MCF}(272\ K)}{k_{RH}(272\ K)} \tau_{MCF}^{OH} \frac{\bar{\chi}_{RH}}{\bar{\chi}_{MCF}} \qquad (18)$$

In this modified equation,

$$\bar{\chi}_i = \frac{\int_{h=0}^{\infty} \rho(h)[X_i(h)/X_i(h=0)]\, dh}{\int_{h=0}^{\infty} \rho(h)\, dh} \qquad (19)$$

where i refers to either MCF or the substance under estimation, $\rho(h)$ is the altitude profile of air density,[65] and $X_i(h)$ are the volume mixing ratios as a function of altitude. Using eq 19, we estimate $\bar{\chi}_{MCF} = 0.94$ on the basis of measurements[63,64] of its vertical distribution, $X_{MCF}(h)$. For a uniformly distributed substance (i.e., with no stratospheric sink), $\bar{\chi}_{RH} = 1$ and the corrected lifetime is slightly longer than that which would be calculated by eq 17. The second correction is due to differences in stratospheric removal by OH for MCF and the substance under estimation, which arise because of their different stratospheric profiles. Because of the vertical temperature[65] and OH concentration[57] profiles, this additional loss takes place mainly above 25 km. Hence, it is negligible for strongly photolyzed chemicals such as MCF but can be as high as 10% for uniformly distributed gases, resulting in a lowering of the lifetime from that calculated by eq 17 alone, which does not include any stratospheric loss. In the cases of most HFCs and HCFCs, these two corrections offset and eq 17 yields a very good approximation of the atmospheric lifetime associated with reaction with tropospheric OH. The value of the global atmospheric lifetime can, thus, be estimated using τ_{RH}^{OH} together with lifetimes associated with losses due to stratospheric photolysis and to oceanic removal (as well as any other significant soil or ecosystem losses).

$$(\tau_{RH}^{global})^{-1} = (\tau_{RH}^{OH})^{-1} + (\tau_{RH}^{strat})^{-1} + (\tau_{RH}^{ocean})^{-1} \qquad (20)$$

4. Uses of Atmospheric Lifetimes

4.1. General Considerations

Using the terminology introduced earlier, the rate of change in the concentration of a species in the atmosphere is given by

$$\frac{dC_{RH}^{global}}{dt} = P_{RH}^{global} - L_{RH}^{global} = P_{RH}^{global} - \frac{C_{RH}^{global}}{\tau_{RH}^{global}} \qquad (21)$$

It is this equation that provided the determination of the global lifetime of MCF discussed previously.[49c,51] Thus, the atmospheric lifetime not only specifies the rate of increase (or decline) in the atmospheric abundance of a species, but also specifies its steady-state or equilibrium concentration. This has been and continues to be an important consideration in evaluating the environmental effects of existing industrial chemicals and the potential acceptability of new ones. For example, the observational records of halocarbons in the atmosphere demonstrate the range of time scales required for the concentrations of chemicals with widely differing lifetimes to return to preindustrial values. Thus, the atmospheric lifetime has become an important gage of a chemical's potential role in the environmental issues discussed in the introduction, two of which will now be considered in more detail.

4.2. Stratospheric Ozone Depletion and Global Warming

Concerns about the potential for anthropogenic chemicals to alter the earth's global atmospheric environment have led to the development of indexes or scales for comparing and quantifying the effects of various compounds on the stratospheric ozone layer and on the radiative balance of the atmosphere. Chlorine loading potentials (CLPs), ODPs, GWPs, and halocarbon global warming potentials (HGWPs) were developed for such roles and all scale directly with the lifetime of an atmospheric chemical. The CLP is an index for representing the total amount of chlorine delivered from the troposphere to the stratosphere as a result of emission of a given halocarbon species RH containing n_{RH} chlorine atoms, referenced to the chlorine delivery from an equivalent weight emission of chlorofluorocarbon-11 (CFC-11, $CFCl_3$).[66,67]

$$CLP = \frac{\tau_{RH}^{global}}{\tau_{CFC\text{-}11}^{global}} \frac{M_{CFC\text{-}11}}{M_{RH}} \frac{n_{RH}}{3} \qquad (22)$$

Here, τ_{RH}^{global}, $\tau_{CFC\text{-}11}^{global}$, M_{RH}, and $M_{CFC\text{-}11}$ are the atmospheric lifetimes and molecular weights of the compound under study and CFC-11, respectively. A similar equation can be written for the bromine loading potential, the total bromine delivered to the stratosphere relative to the chlorine delivered by CFC-11. However, chlorine or bromine delivery alone are not the sole quantifiers of ozone depletion. The amount of stratospheric ozone destroyed as a result

of halocarbon emissions also depends on the chemistry of the breakdown of such gases (i.e., where in the stratosphere the halogen is released) and on the subsequent chemistry of the liberated halogen. The need to actually quantify the ozone loss processes themselves, thereby accounting for the spatial variation of halogen release, requires numerical modeling for a proper assessment of relative halocarbon effects and led to the introduction of the ODP.[68−70] The ODP was defined to represent the amount of ozone destroyed as a result of the emission of a gas (integrated over its entire atmospheric lifetime) relative to that resulting from the emission of the same mass of CFC-11.

$$\mathrm{ODP_{RH}} = \frac{\Delta \mathrm{O_3}\ \text{for emission of a unit mass of RH}}{\Delta \mathrm{O_3}\ \text{for emission of a unit mass of CFC-11}} \quad (23)$$

This formulation assumed that the calculation of relative levels of ozone destruction could be achieved with greater reliability using atmospheric models than the calculation of the absolute level of ozone depletion. Indeed, given its initial focus on a class of similar compounds (i.e., the CFCs whose atmospheric loss occurs entirely via stratospheric photolysis), this assumption was reasonably correct. The ratio of projected ozone destruction attributable to such compounds benefited from a cancellation of systematic errors in the calculated rates of the CFC loss processes themselves.

Because of its inherent simplicity, the ODP concept has subsequently been extended to chemicals that have loss processes throughout the atmosphere (such as removal by tropospheric OH) and that release halogen over a range of stratospheric altitudes. Given the use of CFC-11 as a reference, the aforementioned systematic errors are not canceled in such extended applications. Further, the original calculations of relative amounts of ozone destruction were performed using primarily gas-phase chemistry and tended to underestimate ozone losses in the lower stratosphere occurring as a result of heterogeneous reactions. Present day models now include far better representations of mid-latitude and polar vortex heterogeneous chemical processes. A combination of these models and semiempirical methods[71] (which utilize observed atmospheric profiles of ozone destruction and of halocarbon abundances) are being used to better quantify and reduce the uncertainties in the ODPs. Another problem with the (steady-state) ODP definition in eq 23 stems from the fact that the relative effect of a compound's emission on stratospheric ozone changes with time. This occurs because species with different lifetimes accumulate at different rates in the atmosphere; shorter-lived chemicals reach their steady-state concentrations faster, and their short-time ODP is larger than their steady-state ODP. This has required the definition of specific time horizons for model calculations of ODPs.[69,72] Time-dependent ODPs can be used to provide an indication of the effect on the ozone layer of a mix of compounds with differing lifetimes. Thus, the semiempirical time-dependent ODP at any point in the stratosphere at time t is given by

$$\mathrm{ODP_{RH}}(t > t_s) = \left\{\frac{F_{RH}}{F_{CFC\text{-}11}}\right\}\frac{M_{CFC\text{-}11}}{M_{RH}}\frac{n_{RH}}{3}\alpha\frac{\int_{t_s}^{t}\exp\{-(t-t_s)/\tau_{RH}^{global}\}\,dt}{\int_{t_s}^{t}\exp\{-(t-t_s)/\tau_{CFC\text{-}11}^{global}\}\,dt} \quad (24)$$

$$= \left\{\frac{F_{RH}}{F_{CFC\text{-}11}}\right\}\frac{M_{CFC\text{-}11}}{M_{RH}}\frac{n_{RH}}{3}\alpha\frac{\tau_{RH}^{global}}{\tau_{CFC\text{-}11}^{global}}\frac{1-\exp\{-(t-t_s)/\tau_{RH}^{global}\}}{1-\exp\{-(t-t_s)/\tau_{CFC\text{-}11}^{global}\}}$$

where $\{F_{RH}/F_{CFC\text{-}11}\}$ is the measured fraction of the halocarbon species RH injected into the stratosphere that has been dissociated relative to that of CFC-11.[73] The terms τ_{RH}^{global}, $\tau_{CFC\text{-}11}^{global}$, M_{RH}, and $M_{CFC\text{-}11}$ are as defined for eq 22; n_{RH} is the number of chlorine or bromine atoms in the molecule; t_s is the time required for the molecule to be transported from the troposphere to the region of the stratosphere in question; and α is a factor required for bromocarbons to account for the higher efficiency of bromine to catalyze ozone loss compared with chlorine.

The development of the GWP as an index of relative greenhouse efficiency has followed a track similar to that for the ODP.[69] As in the case of ozone depletion, one can more accurately calculate the relative alterations in radiative forcing associated with two gases than the absolute climate response due to a change in the abundance of one gas alone. The GWP has been defined[3,74] as the ratio of the time-integrated radiative forcing from the instantaneous release of 1 kg of a trace substance RH relative to that of CO_2:

$$\mathrm{GWP_{RH}}(TH) = \frac{\int_0^{TH} a_{RH}[RH](t)\,dt}{\int_0^{TH} a_{CO_2}[CO_2](t)\,dt} \quad (25)$$

where TH is the time horizon over which the calculation is being performed, a_{RH} and a_{CO_2} are the radiative forcings per unit mass of the substance under study and of the reference gas, respectively (expressed in W m^{-2} kg^{-1}), and $[RH](t)$ and $[CO_2](t)$ are the time-dependent decays in the abundances of the trace substance and CO_2, respectively, following their pulsed emissions. Given that the concentration of trace gases in the atmosphere are usually expressed as mixing ratios or in molar rather than in mass units, eq 25 can be rewritten as

$$\mathrm{GWP_{RH}}(TH) = \frac{\int_0^{TH}(a_{RH}/M_{RH})[RH](t)\,dt}{\int_0^{TH}(a_{CO_2}/M_{CO_2})[CO_2](t)\,dt} = \frac{\int_0^{TH} a_{RH}M_{CO_2}\exp\{-t/t_{RH}^{global}\}\,dt}{\int_0^{TH} a_{CO_2}M_{RH}[CO_2](t)\,dt} \quad (26)$$

where the M_i's are the molecular weights of the indicated species and the temporal dependence of the compound of interest is assumed to be exponential. The use of CO_2 as the reference gas results in a_{CO_2} being dependent on the background concentration of CO_2, and $[CO_2](t)$ is a complex response function (i.e.,

not a simple exponential decay) that describes the decay of an instantaneous pulse of CO_2.[75]

For examining the radiative forcings of halocarbons, a HGWP was introduced to express the ratio of the steady-state infrared radiative forcing due to the emission of a halocarbon to that of an equivalent emission of CFC-11.[76] This referencing takes advantage of the fact that the time response functions for both the halocarbon and the CFC-11 reference can be approximated as exponential decays. Hence, when integrated to an infinite time horizon, one obtains

$$\mathrm{HGWP}_{\mathrm{RH}} = \frac{\int_0^{\infty} a_{\mathrm{RH}} M_{\mathrm{CFC\text{-}11}} \exp\{-t/\tau_{\mathrm{RH}}^{\mathrm{global}}\}\, \mathrm{d}t}{\int_0^{\infty} a_{\mathrm{CFC\text{-}11}} M_{\mathrm{RH}} \exp\{-t/\tau_{\mathrm{CFC\text{-}11}}^{\mathrm{global}}\}\, \mathrm{d}t} = \frac{a_{\mathrm{RH}}}{a_{\mathrm{CFC\text{-}11}}} \frac{\tau_{\mathrm{RH}}^{\mathrm{global}}}{\tau_{\mathrm{CFC\text{-}11}}^{\mathrm{global}}} \frac{M_{\mathrm{CFC\text{-}11}}}{M_{\mathrm{RH}}} \quad (27)$$

As with the GWP, eq 27 can be integrated over a specified period of time to obtain a time-dependent value of a HGWP.[77,78]

From the previous discussions, we see that the values of CLP, ODP, GWP, and HGWP all scale according to the global lifetime of an atmospheric gas. This lifetime can be associated with a singular process such as removal by reaction with tropospheric OH or with multiple loss processes occurring throughout the troposphere and stratosphere. For chemically reactive trace gases, the lifetime with respect to removal by tropospheric OH is a dominant component of the global lifetime. The following sections will focus on reviewing laboratory measurement methods for determining the OH rate constants for such reactions, from which $\tau_{\mathrm{RH}}^{\mathrm{OH}}$ can be estimated.

5. Laboratory Techniques for Studying OH Reactivity

5.1. Background

As mentioned previously, a precise and accurate laboratory determination of the rate constant for the reaction of an atmospheric trace gas with the OH radical is the first step in the evaluation of the gas' atmospheric lifetime. There are some comprehensive reviews covering the main features of gas kinetic techniques available for such measurements.[17,79−83] Hence, in this paper we will only outline the principal ones to discuss possible sources of errors associated either with the OH rate constant measurements themselves or with their evaluation for atmospheric modeling purposes. In particular, we will emphasize the identification of relatively small errors that have become increasingly important because of the demands of present atmospheric field observations and modeling.

In the laboratory, the determination of a OH reaction rate constant is essentially the determination of the lifetime of one reactant in the presence of another under conditions created in the chemical reactor. These conditions are typically chosen so that the lifetime is short enough to be measured in the laboratory experiment and that the chemistry inside the reactor is simple enough to ensure that the disappearance of the time-varying reactant is due primarily to the reaction of interest. Hence, the conditions in the laboratory chemical reactor are generally less complex than those in the real atmosphere, with the chemical composition of the mixture in the reactor chosen for the pulsed or steady-state production of OH radicals and for eliminating or minimizing the effects of reactions other than the one of interest (R3).

$$\mathrm{OH} + \mathrm{RH} \xrightarrow{k_{\mathrm{RH}}} \mathrm{H_2O} + \mathrm{R} \quad (\mathrm{R3})$$

Laboratory determinations of the rate constant, k_{RH}, can be placed in one of two measurement categories, absolute or relative. Absolute determinations typically involve the direct monitoring of the real-time decay of the concentration of one reactant due to reaction with an excess concentration of another. The rate constant is then derived from the dependence of the characteristic decay time on the concentration of the excess reactant. The absolute value of the rate constant obtained is dependent on the chemical and physical parameters specified in the experiment, and in the absence of contributions from reactions other than R3 to the loss of the time-varying reactant, its net uncertainty can be evaluated from an analysis of the experimental procedure and data scattering.

Most of the recent absolute studies of hydroxyl radical reactions have involved monitoring the change in the OH concentration in the presence of a large excess of the chemical compound of interest (i.e., under pseudo-first-order conditions where [RH] ≫ [OH] and [RH] is not changed because of its reaction with OH). In the absence of any complicating chemistry, the decay of the OH concentration with time due to reaction (R3) is exponential, and the rate constant can be extracted from the experimental data as

$$k_{\mathrm{RH}} = \frac{\partial^2 \ln\{[\mathrm{OH}]_0/[\mathrm{OH}]\}}{\partial t\, \partial[\mathrm{RH}]} \quad (28)$$

where $[\mathrm{OH}]_0$ is the initial OH concentration.

Monitoring the time evolution of OH in the presence of a known excess concentration of RH offers greater experimental simplicity than the reverse situation. First, it does not require knowledge of the absolute concentration of OH, which is more difficult to determine accurately than the concentration of the stable reactant, [RH]. Second, when present in relatively high concentrations (as is required for studies in which OH is the excess reactant), OH undergoes a fast self-reaction.

$$\mathrm{OH} + \mathrm{OH} \xrightarrow{k_2} \begin{cases} \mathrm{H_2O_2} \\ \mathrm{O} + \mathrm{H_2O} \end{cases} \quad (\mathrm{R4})$$

This self-reaction limits the initial concentration of OH in the chemical reactor and, thus, restricts the range of reaction rate constants that can be measured by monitoring the RH decay. In particular, the kinetics of relatively slow reactions (such as many of the reactions of OH with halogenated hydrocar-

bons) is difficult to investigate in this manner. Further, the products of this self-reaction can initiate secondary reactions making the chemical system more complicated and the results less reliable and accurate. Nevertheless, absolute rate constant determinations performed under excess OH conditions have been used successfully for some fast reactions ($k_i > 10^{-11}$ cm^3 molecule^{-1} s^{-1}). For example, the monitoring of the disappearance of alkenes and aldehydes by mass spectrometry has been utilized for determining the rate constants of such reactants in discharge flow experiments.[84,85] While such experiments do not have problems associated with the reactive impurities in the organic compounds under study, their restrictive utility toward fast reactions is a severe limitation. On the other hand, experiments based on the monitoring of OH decays in the presence of excess concentrations of organic reactants can be seriously affected by the presence of reactant impurities, as will be discussed later.

The relative rate technique involves monitoring the change in the concentration of the compound of interest (RH) together with that of a reference compound (RH_{ref}) due to their reactions with OH radicals under conditions of continuous production of OH. Typically, a mixture containing RH, RH_{ref}, and a photolytic precursor of OH is continuously irradiated to maintain a level concentration of OH despite its disappearance due to self-reaction and to reactions with all other components of the mixture. In such a system, it is extremely difficult to determine the absolute concentration of OH due to the complicated chemistry following its photoproduction. Nevertheless, the rates of consumption of both RH and RH_{ref} are proportional to the same OH concentration and their corresponding OH rate constant.

$$\frac{d[RH_i](t)}{dt} = -k_i[RH_i](t)\,[OH](t) \qquad (29)$$

Because the [OH](t) term is the same for both chemicals,

$$\frac{1}{k_{ref}[RH_{ref}](t)}\frac{d[RH_{ref}](t)}{dt} = \frac{1}{k_{RH}[RH_{RH}](t)}\frac{d[RH](t)}{dt} \qquad (30)$$

and

$$\frac{d\ln[RH](t)}{d\ln[RH_{ref}](t)} = \frac{d\ln\{[RH]_0/[RH](t)\}}{d\ln\{[RH_{ref}]_0/[RH_{ref}](t)\}} = \frac{k_{RH}}{k_{ref}} \qquad (31)$$

where $[RH]_0$ and $[RH_{ref}]_0$ are the initial concentrations of RH and RH_{ref}, respectively. Thus, the ratio of the OH rate constants for the two compounds can be determined from the ratio of the slopes of the time dependences of the RH and RH_{ref} concentrations.

5.2. Absolute Rate Techniques

As discussed previously, most absolute determinations of OH reaction rate constants have involved measurement of the temporal profile of OH disappearance in the presence of an excess concentration of a stable molecular reactant, RH. Thus, the determination of the absolute value of the rate constant requires accurate and precise measurements of two parameters: the absolute concentration of the stable reactant, [RH], and the rate of decay of the reactive transient, OH (see eq 28).

The concentration of the excess reactant can be determined either from a mixture preparation (dilution) procedure or by direct (generally spectral) measurements of its concentration in the mixture in the reactor. Thus, the precision of the concentration determination depends on the precision of the associated pressure, flow, or absorption measurements. The derived errors are typically quite small unless the reactant exhibits some degree of instability in the reactor due to decomposition, adsorption at the reactor surfaces, and so forth.

In general, there are two experimental approaches for obtaining the temporal profile of the OH disappearance due to the reaction of interest: the flow technique and the pulsed technique. In a flow experiment, all measurements are performed in a steady flow of the mixture containing both OH and RH in a long, usually tubular reactor. OH radicals are continuously generated (often via microwave discharge) at the entrance of the reactor, and the second reactant is subsequently added to the flow. Thus, the reaction takes place along the length of the reactor, and the distance from the reactant mixing point to the OH detection region defines the reactant contact time (i.e., the reaction time coordinate). The OH concentration at any particular point along the flow tube does not change with time; that is, the mixture is in a reactive steady state at each distance from the mixing zone. Hence, by measuring the OH concentration at different distances from the mixing zone one can obtain the temporal profile of [OH], its dependence on the concentration of the other reactant, and the rate constant for the reaction. In a pulsed experiment, the degradation of the initial concentration of OH, created in the reactor by the pulsed (i.e., flash or laser) photolysis of a precursor, is monitored in real time. The change in the [OH] temporal decay due to the presence of different amounts of the second compound allows the reaction rate constant to be determined. One of the principal advantages of a pulsed technique over a flow one is the elimination of wall reactions because conditions can be chosen so that the pulse-generated hydroxyl radicals have insufficient time to diffuse to the reactor walls during the measurement of their temporal profile.

5.2.1. Low-Pressure Discharge Flow Technique

A detailed illustrated description and analysis of the low-pressure discharge flow technique have been given by Kaufman[81] and Howard.[79] This technique was, in fact, among the first to be used for the investigation of OH reactions.[86] An important advantage lies in its substitution of steady-state measurements of the hydroxyl concentration for time-dependent ones thereby making a "time-to-space" replacement. Thus, the three essential steps of a rate constant measurement (the generation of the initial

OH concentration, its mixing and reaction with the compound of interest, and the detection of the OH concentration at various time intervals) can be spatially separated. This allows one to simplify or avoid some of the technical and chemical problems associated with such measurements.

To generate OH (or any other radicals for kinetic measurements), the chemical system is often exposed to a high-energy physical process to break chemical bonds and produce the free radicals (such as irradiation by high-energy photons, microwave and electrical discharge, etc.) Such exposure can be a source of error in both pulsed and relative rate experiments as a result of thus initiated unwanted chemistry. In a flow experiment, the hydroxyl radical can usually be generated separately, before the second reactant is added to the flow. This allows for a "clean" radical source, which does not affect the second reactant. Kaufman and Del Greco[87] introduced a fast reaction between H atoms and NO_2

$$H + NO_2 \rightarrow OH + NO \qquad (R5)$$

which became a convenient source of hydroxyl for decades in discharge flow studies of OH reactions. Another fast reaction, which has been occasionally used to generate OH in flow experiments, is

$$F + H_2O \rightarrow OH + HF \qquad (R6)$$

Both reactions R5 and R6 are very fast thereby allowing OH generation (H or F disappearance) to reach completion well before the injection point for the reactant under study. Atomic hydrogen or fluorine can be easily produced in an electrodeless discharge.

Because the reaction between OH and the second reactant takes place in a reactor that is essentially separated from the OH production zone upstream and the OH detection zone downstream, it is technically possible to accurately maintain the desired reaction temperature along the entire reactor. In fact, flow experiments have been performed at most temperatures of atmospheric interest as well as at considerably higher temperatures. The gas mixture attains the temperature of the reactor walls very quickly upon entering the thermostated region in a conventional low-pressure flow apparatus. Thus, the potential error in the rate constant associated with an uncertainty in the reaction temperature can be minimized.

However, the low pressure in the flow reactor (on the order of a few hundred Pascals or a few Torr) can be a disadvantage of this technique. In studies of simple H-atom abstraction reactions, the low-pressure limitation does not pose a problem. However, this technique becomes restrictive when the OH reaction is pressure-dependent or proceeds through the formation of an intermediate adduct. Reactions of OH with CO and HNO_3 are examples of important pressure-dependent atmospheric processes, which have required measurements at atmospheric pressures.[57] The high-pressure turbulent flow technique[88] (discussed subsequently) permits measurements at such higher pressures.

One of the main advantages of a flow technique is that steady-state concentrations of radicals are measured. This allows an integration time period for the detection system suitable for achieving the desired sensitivity and signal-to-noise ratio. For example, electron paramagnetic resonance (EPR)[89−94] and laser magnetic resonance (LMR)[95,96] techniques, which are very selective and sensitive toward OH, can only be used in a flow experiment because of the long integration times required. In addition, the higher pressures typically used in pulse experiments to minimize molecular diffusion results in pressure broadening of the far IR absorption lines used in LMR, resulting in a substantial loss in sensitivity. Detection techniques based on stimulated OH ultraviolet fluorescence (resonance fluorescence, RF, and laser-induced fluorescence, LIF) also benefit from much longer signal integration times when compared with their use in real-time pulsed experiments.

Variation of the reaction time in flow experiments is usually accomplished by varying the distance between the detector and the reactant mixing zone. Use of a movable injector for the introduction of the hydroxyl radicals or of the excess stable reactant in a flow experiment helps to minimize some problems associated with this technique. Some detection techniques (EPR, LMR) have a sizable detection zone with nonuniform sensitivity. The use of a movable injector allows one to avoid an additional error associated with this fact, even if the detection zone length is comparable to the reactor length.[97]

A movable OH injector allows one to quantify the wall loss of hydroxyl radicals, which is necessary for accurately correcting the experimental data for the effects of diffusion processes in the reactor. Using a fixed OH source and a movable inlet (or a series of fixed inlets) for the excess reactant does not enable one to quantify such OH heterogeneous removal. This may create the illusion that heterogeneous processes have, in fact, been avoided in the experiments.

To a first approximation, a low-pressure flow experiment converts the reaction time to a distance within the reactor according to very simple expression:

$$t = z/v \qquad (32)$$

where t is the reaction time, z is a distance between the reactant mixing point and the detection zone, and v is the average gas flow velocity in the reactor. This so-called *plug flow* assumption allows the use of a simple equation to describe the [OH](z) evolution

$$v\frac{\mathrm{d}[OH](z)}{\mathrm{d}z} = -(k_{\mathrm{wall}} + k_{\mathrm{RH}}[\mathrm{RH}])[\mathrm{OH}](z) \qquad (33)$$

where k_{wall} is a OH decay rate due to collisions with the flow reactor walls and to reactions with impurities in the carrier gas.

In reality, neither the flow velocity nor the radical concentration, [OH], are uniform across the flow reactor. Thus, the [OH] profile along the flow reactor cannot always be simply recalculated into its temporal profile using the simple plug flow assumption. Instead, the reactant concentration profile should

obey the continuity equation, which can be represented in the case of an isothermal gas of constant density flowing along an azimuthally symmetric tubular reactor as

$$v(r)\frac{\partial[\mathrm{OH}](r,z)}{\partial z} = \nabla\{D(r) \times \nabla[OH](r,z)\} - k_{\mathrm{RH}}[\mathrm{RH}][\mathrm{OH}](r,z) \quad (34)$$

where r and z are the radial and axial coordinates, respectively; $v(r)$ is the axial gas flow velocity; $D(r)$ is the diffusivity of OH in the gas mixture; [OH](r, z) and [RH] are the concentrations of hydroxyl and excess reactant, respectively; and k_{RH} is the rate constant for the reaction between them. All low-pressure flow experiments are performed under conditions of fully developed laminar flow, that is, when

$$Re = 2R_0\bar{v}\rho/\eta < 10^3 \quad (35)$$

where Re is a parameter called the Reynolds number, R_0 is the radius of the tube, $\bar{v}$ is the average axial velocity of the flow, ρ is the gas density, and η is the viscosity of the gas. In this case, the axial flow velocity attains a parabolic radial profile (within a 1% error) at the length z_{pois} of the tubular reactor[98]

$$z_{\mathrm{pois}} \cong 0.23{R_0}^2\rho\,\bar{v}/\eta = 0.115R_0Re \quad (36)$$

and the continuity equation for fully developed steady-state Poiseuille flow can be rewritten as

$$2\bar{v}\left\{1 - \frac{r^2}{{R_0}^2}\right\}\frac{\partial[\mathrm{OH}](r,z)}{\partial z} = D\left\{\frac{\partial^2[\mathrm{OH}](r,z)}{\partial r^2} + \frac{1}{r}\frac{\partial[\mathrm{OH}](r,z)}{\partial r} + \frac{\partial^2[\mathrm{OH}](r,z)}{\partial z^2}\right\} - k_{\mathrm{RH}}[\mathrm{RH}][\mathrm{OH}](r,z) \quad (37)$$

Thus, *a laminar flow discharge technique* is a more proper name for the conventional low-pressure discharge flow technique. A number of studies have been devoted to the analysis of this last expression to accurately treat the results of observations obtained under laminar flow conditions[99−104] with various boundary conditions dictated by the probability of OH removal due to collisions with the reactor walls. Note that the diffusion eq 37 describes first-order kinetics quite well in the case of laminar flow and can be solved and analyzed by a variety of numerical and analytical techniques. This allows, in principle, an accurate analysis of the data obtained under certain experimental conditions. It also allows one to define the experimental conditions under which the correct value of the reaction rate constant can be accurately obtained despite more or less pronounced effects of diffusion-controlled processes.

Sufficiently far downstream from the mixing region, the concentration of the active reactant (OH) decreases exponentially with distance along the tubular reactor. It is this purely exponential decay that allows for the rate constant determination from a flow experiment. The measured spatial distribution of the hydroxyl concentration along the flow reactor, [OH](z), is caused by both the OH removal in chemical processes and its diffusion due to the concentration gradients. The analysis of the diffusion equation is necessary for correct transformation of the experimentally measured axial [OH](z) decay profile under particular flow conditions to the time dependence of hydroxyl concentration, [OH](t), due to chemical process.

The simple plug flow assumption is valid when diffusion is fast enough so that neither wall removal of OH nor the Poiseuille velocity distribution can cause the radial gradient of the OH concentration. Under such conditions, eq 32 is correct if the flow velocity is high enough to prevent the distortion of the axial profile of [OH] due to diffusion along the reactor axis. To account for this later effect of axial diffusion and obtain the correct value of k_{RH}, the effective first-order decay rate determined under the plug flow assumption, τ_{pf}^{-1}, should be corrected as follows:[99]

$$k_{\mathrm{RH}}[\mathrm{RH}] + k_{\mathrm{wall}} = \tau_{\mathrm{pf}}^{-1}\left(1 + \frac{\tau_{\mathrm{pf}}^{-1}D}{v^2}\right) \quad (38)$$

The wall removal of OH poses additional problems by increasing the radial gradient of the radical concentration. This becomes more important as the rate of the heterogeneous process increases and as pressure in the reactor increases. A widely used computing algorithm was presented by Brown[102] to correct the measured decay rate, τ_{pf}^{-1}, for the effects of both radial and axial diffusion to obtain the correct value of k_{RH}. In general, flow experiments are performed under conditions where diffusion effects are not very pronounced, so that only small corrections need be made to obtain the accurate values of the rate constants. These corrections are minimized by the use of low pressures in the reactor and a high gas flow velocity.

OH removal due to collisions with reactor walls is usually minimized by coating the reactor surface with halocarbon polymer films or wax. The OH wall loss, measured as the OH decay rate in the absence of the excess reactant, is implicitly assumed to be constant and independent of the reactant concentration. However, the real nature of the heterogeneous loss is never known and adsorbed reactant on the surface can be involved.[105] Heterogeneous reactions can manifest themselves through a poor reproducibility of the results,[106,107] especially at low temperatures.[94] A noticeable curvature of the Arrhenius plot at low temperatures can also be indicative of such complications. To confirm the homogeneous nature of the process under study, one should conduct test experiments in reactors of different diameters, thereby varying the surface-to-volume ratio of the reactor. However, even this is not totally sufficient because the use of different reactors means a change in the surfaces themselves. Despite sporadic use of various diameter reactors in the study of the OH reactivity,[108,109] the homogeneous nature of the OH removal is usually assumed. Note that the analysis of the continuity equation allows the technique to separate

between homogeneous and heterogeneous components of the reaction under study in a flow experiment performed at different pressures.[105]

The demand for higher pressure data and the potential problem of wall reactions stimulated the conduct of high-pressure measurements under flow conditions. Keyser[108] successfully used a discharge laminar flow technique to study the OH reaction with HCl at room temperature at helium pressures up to 100 Torr (13 kPa). Nevertheless, the laminar flow experiment cannot generally be used to study OH reactions at high pressure and atmospheric temperatures because the mixing time and the time needed for the gas flow to attain the reactor wall temperature become too long. Both processes are controlled by radial diffusion, and its characteristic length in the Poiseuille flow, z_{diff}, is determined by the solution of the diffusion eq 37

$$z_{diff} \cong 0.27R_0^2\bar{v}/D \cong 205R_0^2\bar{v}P(\text{atm})/D_0, \quad \text{cm} \quad (39)$$

where D_0 is the diffusion coefficient in the mixture at 1 atm (101 kPa) and P(atm) is the pressure in the reactor. To perform such measurements by a flow technique, the radial mixing process should be forced somehow. This has been accomplished by allowing microturbulence in the reactor.

5.2.2. High-Pressure Turbulent Flow Technique

The first kinetic results obtained in a turbulent flow reactor were high-temperature data published by Westbrook et al.[110] A comprehensive analysis of the use of this experimental approach in studying the elementary reactions of free radicals was performed by Abbatt et al.,[112] Seeley et al.,[111] and Donahue et al.[115] In contrast with a conventional laminar flow technique, this approach is complicated by the lack of a correct ab initio mathematical description of the flow in the reactor. In the case of laminar flow, the continuity eq 37 can be analyzed on the basis of the macro parameters of the flow: pressure, average flow velocity (total gas flow), and diffusion coefficient. In the case of turbulent flow, neither the radial distribution of flow velocity, $v(r)$, nor $D(r)$ are known in eq 34. A turbulent gas flow consists of a fast-moving central core, which is well-mixed due to microturbulence, and a slow-moving laminar sublayer near the reactor walls, which mixes by slow molecular diffusion at the high gas pressure. Further details on this technique can be found in the references cited previously.

The plug flow approach has actually been accepted for use in the determination of reaction rate constants based on data obtained in a turbulent flow experiment. The distribution of the flow velocity across the reactor (which is not perfectly flat)[110,111,115,119] should be measured experimentally to establish the effective flow core velocity, v_{eff}, to be used in eqs 32 and 38. Thus determined, v_{eff} can exceed the average flow velocity in turbulent flow so that $v_{eff}/\bar{v}$ can be as high as 1.1−1.3 and approach unity at very high Reynolds numbers.[111,119] Gas mixing inside the flow core is mainly due to microturbulence, and the corresponding "eddy" mixing coefficient, D_{eff}, should also be determined experimentally for use in eq 38[111,119] to correct the derived rate constant for axial mixing. Seeley et al.[111] determined the average value of D_{eff} for their particular turbulent reactor to be about 250 cm^2/s (the range is 50−500 cm^2/s) and independent of the Reynolds number.

Despite fast eddy mixing inside the core of the flow, the existence of a laminar sublayer near the reactor walls (which is slow mixing at high pressure) can essentially suppress the wall removal of free radicals.[111] Therefore, a principal disadvantage of the low-pressure flow technique is drastically reduced. A turbulent flow technique permits the realization of the advantages of a flow technique under its simplest plug flow conditions for rate constant measurements at pressures and temperatures of atmospheric interest with little concern about the possible influence of wall reactions.

Abbatt et al.[112] used a turbulent flow reactor with LIF detection to study OH reactions of atmospheric interest at room temperature. The technique was used in both laminar and turbulent regimes at Reynolds numbers from 1200 to 37 000. The experiments were performed at helium pressures up to 380 Torr (51 kPa) in a tubular flow reactor of about 12-cm i.d.. These measurements were later extended to higher[113] and lower temperatures of atmospheric interest[114] over a pressure range of 2 Torr (270 Pa) to 600 Torr (80 kPa) of nitrogen.[115,116] The high-pressure turbulent flow technique has also been used for low-temperature measurements of Cl atom[117] and HO_2 radical reactions[118,119] in a 2.5-cm i.d. reactor coupled with RF,[117] mass spectrometry,[118] and tunable diode laser absorption[119] detection techniques.

The most serious experimental drawback of the turbulent flow technique is the enormous amount of carrier gas needed to form the high Re flow. Also, the formation of fully developed turbulent flow may require a distance in the reactor as long as $200R_0$.[120,121] Therefore, the region of turbulent flow in the reactor should be determined experimentally. In contrast with the conventional laminar flow technique, the average effective velocity of the turbulent core should be determined from the measured radial profile of the velocity, which still has a maximum in the central part despite turbulence. Such measurements can be done using the Pitot tube technique[111,112,119] with an uncertainty of about 5%,[111,115,119] which thus becomes one of the main instrumental uncertainties of this technique for the measurement of accurate rate constants. Another minor concern is the uncertainty of the "eddy" mixing coefficient, D_{eff}, which determines the correction for axial mixing (eq 38) and for possible complications from "nonperfect" radial mixing. The slow mass exchange between the core of the flow and that near the wall, which helps in preventing the OH wall reactions, also restricts the wall-to-core temperature exchange. Therefore, caution must be taken to verify the gas temperature when conducting low-temperature measurements.

5.2.3. Pulsed (Flash or Laser) Photolysis Technique

A pulsed photolysis technique is, in principle, the most "direct" way of studying the reactivity of free

radicals by monitoring their reactive disappearance in real time. First introduced by Norrish and Porter,[122] the technique has become one of the most powerful and widely used means to study gas-phase reactions. The technique was first employed to study an atmospheric OH reaction 40 years ago when Husain and Norrish[123] determined the rate constant for the reaction between OH and HNO_3. UV absorption spectroscopy using photographic plates was employed to monitor the evolution of the OH concentration in early flash photolysis studies.[123,124] It was later replaced by absorption measurements using OH resonance radiation from a microwave discharge on a flowing mixture of H_2O diluted with He,[125] which allowed a faster, more sensitive, real-time monitoring of the OH decay. The "resonance" radiation emitted by the hydroxyl radicals electronically excited in the microwave discharge, $OH(A^2\Sigma^+)$, matches the absorption spectrum of the hydroxyl radical ground state, $OH(X^2\Pi)$, to be detected, thereby increasing the detection sensitivity. The flash photolysis technique further benefited from the introduction of highly sensitive OH fluorescence detection methods: RF and LIF.

The RF detection of OH in a room temperature pulsed system was first used by Stuhl and Niki[126,127] and shortly later by Kurylo,[128] while a temperature-varying capability was first added by Davis et al.[129] and Perry et al.[130] The intensity of the hydroxyl radical fluorescence (and, hence, the sensitivity of the OH detection technique) depends on the intensity of the pumping radiation causing OH excitation into its upper electronic state ($A^2\Sigma^+$) and on the quenching rate of $OH(A^2\Sigma^+)$ due to molecular collisions in the reactor. The last factor decreases the sensitivity of RF at higher pressures and high concentrations of reactant. The use of laser radiation to stimulate the OH fluorescence (LIF) improved the sensitivity of the detection technique.[131,132] The high intensity of laser radiation allows one to saturate the $OH(X^2\Pi) \leftrightarrow OH(A^2\Sigma^+)$ transition, resulting in a pressure-independent sensitivity of LIF detection. This permits the conduct of OH reaction studies at pressures as high as 150 atm (1.5×10^4 kPa).[133] Whereas typical determinations of atmospheric lifetimes do not require OH rate-constant measurements above 1 atm (10^2 kPa) pressure, such studies can be useful in determining reaction mechanisms and branching ratios.

Details of these detection techniques can be obtained from the original papers and reviews.[17,80,81] As a result of their high sensitivity toward OH, fluorescence techniques have become the main detection tools for OH reactivity studies in both pulsed photolysis and discharge flow techniques, with the majority of work being performed using LIF detection. Both techniques require measurement of the radiation re-emitted by the hydroxyl radicals after their excitation by a source of continuous resonance radiation (RF) or by a short pulse of narrow wavelength band laser radiation (LIF). As mentioned previously, the continuous source of resonance radiation in the RF technique is a microwave discharge in an H_2O-containing flow of inert gas (typically He or Ar). The radiation from electronically excited $OH(A^2\Sigma^+)$ in the discharge plasma is absorbed by OH in the reactor and subsequently detected as $OH(X^2\Pi) \leftarrow OH(A^2\Sigma^+)$ fluorescence. This fluorescence near 309 nm comes from the 0−0 vibrational band and is detected on an axis perpendicular to the incident radiation as a relative measure of the OH concentration. Because both the relatively intense radiation from the discharge lamp and the very weak fluorescence radiation are in the same wavelength range, proper collimation is important in improving detection sensitivity, which depends on the absolute intensity of the OH fluorescence and its ratio to the intensity of the incident radiation scattered by reactor surfaces and by the bath gas in the reactor (Rayleigh scattering).

Two approaches have been used for the LIF detection of OH. Tully and co-workers[132,134] employed a quasi-continuous wave (CW) laser system to pump hydroxyl radicals in the 0−0 band of the $OH(X^2\Pi) \rightarrow OH(A^2\Sigma^+)$ transition near 308 nm[132] or 307 nm.[134] The very narrow laser line width (ca. 1.6×10^{-5} nm) falls within the absorption bandwidth of a single rotational−vibrational transition, thus minimizing nonusable radiation and maximizing the ratio of the OH fluorescence to scattered radiation. The use of a CW laser system[132,134] instead of a conventional "resonance" discharge lamp[135] provided more than 1 order of magnitude improvement in the OH detection sensitivity. In addition, the much better collimated laser radiation greatly reduced scattered radiation compared with that from a discharge resonance lamp.[132] The CW variant of the LIF detection technique is methodologically similar to the RF technique in that continuous monitoring of [OH] following each production pulse is employed.

The most widely used variant of LIF detection is that of pulsed LIF.[131] Using a single-pulse laser, the OH concentration is measured at a particular reaction time (i.e., the delay time between the pulsed photolytic production of OH and the pulse of the monitoring laser). The entire temporal profile of the hydroxyl decay under the particular conditions in the reactor is obtained by conducting many consecutive pulsed experiments with different delay times. Laser line-narrowing techniques have been used to obtain spectral line widths as small as 0.001 nm,[136] which is comparable with the Doppler broadened absorption spectral line width of about 4×10^{-4} nm. This provides similar increases in the signal-to-noise ratio, as discussed for CW LIF detection.

The high intensity of a pulse laser allows pumping of the OH absorption band corresponding to the ($X^2\Pi$, $v = 0$) → ($A^2\Sigma^+$, $v = 1$) transition near 282 nm, well shifted from the 309 nm region of OH fluorescence in the 1−1 and 0−0 bands of the $(A^2\Sigma^+) \rightarrow (X^2\Pi)$ transition. Thus, any scattered laser radiation can be further attenuated by the placement of a narrow band-pass interference filter in front of the detection photomultiplier. The advantages of laser pumping of the OH excited state has made LIF the most sensitive and widely used technique to detect hydroxyl radicals in laboratory studies as well as in the real atmosphere.[137,138] The LIF technique also provides excellent time resolution without any compromise between

resolution and sensitivity because the duration of the detection laser pulse is extremely short (usually, less than ca. 10−20 ns).[139] The duration of the laser photolysis pulse is similar. The radiative lifetime of the upper state of hydroxyl, OH ($A^2\Sigma^+$), another limiting parameter, is on the order of 1 μs for the ($A^2\Sigma^+$, $v = 0$) → ($X^2\Pi$, $v = 0$) and ($A^2\Sigma^+$, $v = 1$) → ($X^2\Pi$, $v = 1$) transitions,[140] which are used for monitoring the hydroxyl concentration in the RF and LIF techniques. This limit is lowered in higher pressures experiments when the collisional quenching by molecules of bath gas and reactant makes the OH ($A^2\Sigma^+$) lifetime even shorter. Thus, LIF offers better than 1-μs time resolution. It can, however, be degraded by longer scattered fluorescence from the reactor walls and collimating optics.

For both RF and LIF detection, repetitive pulsed experiments are needed to accumulate the OH signal to obtain an acceptable signal-to-noise ratio and a OH decay curve of higher precision. However, a temporal profile of the OH decay is obtained by two different ways using these techniques. LIF is a multipulse technique by its very nature, as described previously. Therefore, pulse-to-pulse instability of both the photolysis and the detection laser pulses can contribute to LIF signal noise. However, both pulse energies can be measured to correct the fluorescence signal. When RF detection is used, an entire kinetic decay of OH can be acquired following each pulsed initiation, and the sole purpose of accumulating the signal from multiple experiments is for improving the signal-to-noise ratio.

In contrast with the discharge flow technique discussed previously, the pulsed generation of OH in the presence of the compound to be studied is a possible source of error in a pulsed (especially flash) photolysis experiment. Specifically, the radiation used for pulsed photolysis of a OH precursor can also dissociate the stable reactant. Products of such photolysis can react with OH, contributing to its temporal decay and causing an error in the rate constant derived. This is why a number of precursors and pulsed radiation sources are often used. Discharge flash lamps are the simplest sources of UV radiation that can be used to dissociate H_2O, HNO_3, and H_2O_2 and directly produce OH radicals. The photolysis of water using pulsed radiation from a Xe flash lamp

$$H_2O + h\nu \text{ (Xe lamp} < 185 \text{ nm)} \rightarrow OH + H$$

is a very attractive source of hydroxyl because OH is the immediate product of photolysis, and it does not react with the precursor. However, as mentioned previously, the short wavelength radiation can dissociate the reactant. This problem also exists when a F_2 excimer laser operating at 158 nm is used for the dissociation of H_2O. Nevertheless, properly selected pulsed lasers are widely used as the radiation source. The very short laser pulse can be easily collimated in the cell, thereby decreasing scattered light from the OH generation process. In addition, the use of pulsed lasers allows the determination of the initial OH concentration from the pulse energy, the precursor concentration, and the absorption cross section. Such quantification is very difficult when a discharge flash lamp is used. Excimer lasers generating at 193 nm (ArF), 248 nm (KrF), and 351 nm (XeF), as well as the fourth and third harmonics of a Nd:YAG laser at 266 and 355 nm, respectively, are the most common pulse radiation sources. They have been used to directly generate OH

$$H_2O_2 + h\nu \text{ (193 nm, ArF*; 248 nm, KrF*; 266 nm, Nd:YAG, } 4\omega_0) \rightarrow OH + OH$$

$$HONO + h\nu \text{ (351 nm, XeF*; 355 nm, Nd:YAG, } 3\omega_0) \rightarrow OH + N$$

$$HNO_3 + h\nu \text{ (248 nm, KrF*)} \rightarrow OH + NO_2$$

or to produce electronically excited oxygen atoms, $O(^1D)$

$$N_2O + h\nu \text{ (193 nm, ArF*)} \rightarrow O(^1D) + N_2$$

$$O_3 + h\nu \text{ (248 nm, KrF*; 266 nm, Nd:YAG, } 4\omega_0) \rightarrow O(^1D) + O_2$$

which immediately react with any added H-atom donor (H_2O, H_2) or even the reactant under study to produce hydroxyl radicals. Two-photon dissociation of NO_2 has also been used to produce $O(^1D)$ at even longer wavelengths (ca. 410−450 nm) using a dye laser pumped by the third harmonic of a Nd:YAG laser:[141]

$$NO_2 + h\nu \text{ (410−450 nm, Nd:YAG, } 3\omega_0 + \text{dye}) \rightarrow O(^1D) + NO$$

The use of different sources of OH allows one to examine any effects of the hydroxyl source on the derived OH rate constant. These different OH generation methods also allow the use of longer wavelength radiation, which generally results in less photolysis of the reactants,[142,143] although such use can complicate chemistry in the reacting mixture because of the reaction between OH and its precursors. Thus, extreme care must be taken to ensure that the measured OH rate constants are not affected by complications due to reactant photolysis or OH reactions with its precursors.

The photolysis pulse creates an initial concentration of hydroxyl radicals along the center of the reactor. This OH concentration degrades due to chemical reactions and diffusion out of the irradiated zone. While reaction with the compound under study, with any OH precursors, or with reactive impurities would result in a simple exponential decay at any location in the reactor, diffusion tends to level the initially created OH spatial distribution. Thus, the role of diffusive OH transfer should be analyzed to avoid even minor possible complications. In the majority of pulsed experiments, the experimentally obtained temporal profiles of the signal are reported to follow a simple exponential decay within the data scattering and the presentation of the kinetic results

is based on a simple equation to describe the [OH](t) evolution

$$\frac{d[OH](t)}{dt} = -(k_{diff} + k_{RH}[RH])[OH](t) \quad (40)$$

where k_{diff} is a OH decay rate due to the diffusion out of the detection system viewing zone and reactions with impurities and precursor in the reactor.

However, the change in OH concentration due to diffusive degradation of the pulse-generated core is generally nonexponential, in contrast with the flow case. As stated earlier, a principal benefit of a pulsed experiment is that the measurements are made over a time scale shorter than the time required for OH to diffuse from the irradiated zone to the walls of the reactor. Therefore, a steady-state radical distribution (steady-state solution of the continuity equation) is not applicable to describe the pulse experiment. From a mathematical point of view, this is the principal difference between flow and pulsed experiments and may cause some complications when the OH rate constant is extracted from the experimentally obtained OH temporal profile. To illustrate this, we can recall the continuity equation, which describes the evolution of the OH distribution due to diffusion and reactions:

$$\frac{\partial[OH](x_i, t)}{\partial t} = D \times \nabla^2[OH](x_i, t) - \{\tau_0^{-1} + k_{RH}[RH]\}[OH](x_i, t) \quad (41)$$

where x_i are space coordinates and τ_0^{-1} is the OH decay rate due only to reactions with precursors and impurities. The solution of eq 41 with initial conditions preset by the instantaneous pulsed generation of OH dictates the temporal profile of the detected signal. Due to the linearity of eq 41, its solution can be obtained as

$$[OH](x_i, t) = [OH]_{diff}(x_i, t) \exp\{-(\tau_0^{-1} + k_{RH}[RH])t\} \quad (42)$$

where $[OH]_{diff}(x_i, t)$ describes the evolution of the OH concentration due to diffusion only, that is, a solution of the following equation:

$$\frac{\partial[OH](x_i, t)}{\partial t} = D \times \nabla^2[OH](x_i, t) \quad (43)$$

The temporal profile of $[OH]_{diff}(x_i, t)$ can be illustrated by the solution of eq 43 for the simplest initial conditions of axial symmetry, that is, an initial OH "line" distribution. In this case

$$[OH]_{diff}(r, t) = \frac{L_{OH}}{4\pi Dt} \exp\left\{-\frac{r^2}{4Dt}\right\} \quad (44)$$

where L_{OH} is the number of OH radicals per unit length of the instant line source.[144,145] Even in this simple case, the loss of OH due to diffusion out of the irradiated zone is nonexponential. Rather, [OH] decreases as $1/t$ at a small distance from the source. In reality, the fluorescence signal, $I(t)$, is a function of both the OH distribution and the spatial apparatus sensitivity function, $\Phi(x_i)$

$$I(t) = \int_V [OH](x_i, t)\, \Phi(x_i)\, dV = \int_V [OH]_{diff}(x_i, t) \exp\{-(\tau_0^{-1} + k_{RH}[RH])t\} \Phi(x_i)\, dV = \exp\{-(\tau_0^{-1} + k_{RH}[RH])t\} \int_V [OH]_{diff}(x_i, t)\, \Phi(x_i)\, dV = I_{diff}(t) \exp\{-(\tau_0^{-1} + k_{RH}[RH])t\} \quad (45)$$

where $I_{diff}(t)$ is the fluorescence signal temporal profile due to diffusion only and is obviously not exponential.

Nonexponential temporal profiles due to OH diffusion out of the detection zone have been observed in some LIF[132,134,146] and RF[147] experiments. To account for such a background decay, Tully and coworkers[132,134,146] used a semiempirical expression in their data treatment. On the basis of the above analysis of the diffusion equation, Orkin et al.[147] proposed a simple procedure to account for the diffusion without any specification of $I_{diff}(t)$. This procedure involves point-by-point treatment of the data obtained in the presence of the reactant, $I_{[RH]}(t)$, and in its absence, $I_0(t)$, to calculate the decay constant due to the reaction of interest only while accounting for the actual shape of the "diffusional" temporal profile. Thus, k_{RH} can be obtained as

$$\frac{1}{[RH]} \frac{\partial}{\partial t} \ln\left\{\frac{I_0(t)}{I_{[RH]}(t)}\right\} = \frac{1}{[RH]} \frac{\partial}{\partial t} \ln\left\{\frac{I_{diff}(t) \exp(-t/\tau_0)}{I_{diff}(t) \times \exp(-t/\tau_0) \exp(-k_{RH}[RH]t)}\right\} = k_{RH} \quad (46)$$

Such data treatment allows one to reliably measure reactive decay rates that are slower than the background rate due to diffusion and yields pseudo-first-order plots with no intercept corresponding to the decay rate in the absence of the added reactant.

A background temporal profile (in the absence of any reactant) depends on several factors, such as the reactor geometry, the geometry of the intersection of the photolysis and detection radiation beams, the presence of reactive impurities and precursors, and the pressure and type of the inert gas in the reactor. In the case of a fast decay rate due to the reaction, the exact shape of the background decay is not important. It becomes increasingly important when the decay rate due to reaction becomes slow due either to a small reaction rate constant or to instrumental restrictions.

5.3. Relative Rate Techniques

The most important advantage of a relative rate technique lies in the monitoring of the disappearance of the stable reactant rather than that of OH radicals. As a result, the rate constants obtained are usually not affected by the presence of reactive impurities in the compound of interest. Based on this fact alone, a relative rate technique is a very useful complement

to absolute techniques in which only the OH concentration is monitored.

However, to obtain the absolute value for a rate constant using the relative rate technique, the rate constant of the reference reaction must be available from independent absolute measurements. Thus, the resultant rate constant accumulates all of the uncertainties associated with the rate constant of the reference reaction in addition to those of the relative rate experiment itself. On the other hand, this feature can be quite advantageous in some cases. As discussed earlier, the "scaling" procedure for estimating an atmospheric lifetime requires the ratio of OH rate constants for the compound of interest and for a well-characterized atmospheric proxy gas such as MCF, as in eq 17. Hence, the use of CH_3CCl_3 as the reference compound in a relative rate experiment results in a direct measurement of this ratio. In such a case, one avoids the need for the absolute determination of the rate constants for either the compound of interest or CH_3CCl_3, as well as the accumulation of the uncertainties associated with each. Moreover, the procedure of obtaining the rate constant ratio does not require measurement of the absolute concentration of either reactant, thereby lending to the increased accuracy of the result.

The experimental approaches for relative rate measurements differ mainly in the compound detection techniques and in the photolytic precursors for OH. Ideally, such measurements should involve small changes in the initial concentrations of the compound of interest and of the reference compound to minimize the formation of the products both from the OH precursor photolysis and from the OH reactions. In addition, because of some physical−chemical issues discussed in the following, a relative rate experiment should be conducted at relatively low initial concentrations of the compounds under study, thus requiring that the detection technique be of high sensitivity and precision. It should also be sufficiently selective to reliably differentiate both compounds from one other and from all other chemicals arising both from the initial photolysis and from OH reactions. It is often difficult to satisfy all these requirements in every case.

There are two main photochemical processes for OH formation that are used in relative rate experiments. The photolysis of water at 184.9 nm (using a mercury lamp)

$$H_2O + h\nu \rightarrow OH + H$$

has been a very attractive source because OH is the immediate photolysis product and does not readily react with the precursor (similar to the advantages associated with H_2O photolysis using a Xe flash lamp in pulsed systems). The other product of the photolysis, the H atom, is far less reactive toward hydrocarbons than OH[148] and is scavenged by traces of (or added) oxygen to form HO_2. Unfortunately, H_2O absorbs only vacuum UV radiation at wavelengths shorter than 190 nm, which is also absorbed by the majority of chemicals of atmospheric interest. This makes this source of hydroxyl most useful for studying OH reactions with alkanes and fluorinated alkanes, which do not absorb radiation at this wavelength.

The problem of reactant photolysis is avoided by using the photolysis of ozone at $\lambda < 310$ nm (the 253.7-nm line from a mercury lamp is a common radiation source) followed by the reaction of the excited oxygen atoms, $O(^1D)$, with a hydrogen-containing compound, usually H_2O, as the OH source.

$$O_3 + h\nu \rightarrow O(^1D) + O_2$$

$$O(^1D) + H_2O \rightarrow OH + OH$$

This longer wavelength radiation is not strongly absorbed by a wide variety of chemical compounds. However, involving an intermediate reaction of a highly reactive species such as $O(^1D)$ causes other possible complications. Both the compound under study and the reference can disappear due to reaction with $O(^1D)$, causing an error in the derived OH rate constant ratio. To avoid this complication, very low radical concentrations must be used.

Other photochemical sources of hydroxyl can be used based on the design of the reactor and absorption spectra of the compounds under study. The photolysis of H_2O_2, HNO_3, or HONO directly produces OH. The photolysis of methyl nitrite in the presence of NO and air (typically in smog chamber studies) results in OH production via the following chemical processes.

$$CH_3ONO + h\nu \rightarrow CH_3O + NO$$

$$CH_3O + O_2 \rightarrow HCHO + HO$$

$$HO_2 + NO \rightarrow OH + NO_2$$

This chain of chemical reactions has been accepted as a standard method for determining the OH rate constants for organic compounds.[149] However, the use of such large molecules as photoprecursors often leads to complex chemistry in the reaction mixture initiated by their reaction with OH itself. In such studies, the consumption of the chemicals under study is often quite appreciable (approaching 80−90%). Thus, the reacting mixture is not only quite complex but changes in composition during the experiment. Extreme caution must be taken to ensure that the rate constant ratio obtained is not affected by the complexity of the chemical system and that reaction with OH is the single sink for both compounds under study. With appropriate care, this method has been used successfully for the measurements of relatively fast reactions. A comprehensive analysis of a OH relative rate technique is given by Atkinson[82] and Brauers and Finlayson-Pitts,[150] (the last paper presents an error propagation analysis).

Relative rate measurements have been performed in reaction chambers of various designs and very different volumes using several detection techniques. There are two principal techniques that are most suitable for tracking the concentrations of the stable reactants in such experiments: Fourier transform infrared spectroscopy (FTIR) using multipass absorp-

tion cells and gas chromatography (GC-MS, GC-FID). Atkinson and Pitts (and co-workers) have used large Teflon bags (75 L−6 m^3) with GC[151,152] and FTIR[153] monitoring of organics for studies at room temperature. They also used a 6-m^3 thermostated environmental chamber[154] for such measurements. Large Teflon bags coupled to a GC detection system were widely used by Sidebottom and co-workers (50-L chamber)[155] and by Wallington and co-workers (100-L chamber).[156] Large-volume reactors made of different materials were also used by Pitts and co-workers (6-m^3 Pyrex smog chamber coupled with GC),[157] Wallington and co-workers (140-L Pyrex reactor coupled with FTIR),[158] Orlando et al. (47-L stainless steel reactor coupled with FTIR),[159] Molina and co-workers (7.6-L Pyrex reactor coupled with FTIR),[160] and Chen et al. (1000-L Teflon coated stainless steel reactor coupled with FTIR[161] and 11.5-L quartz reactor coupled with GC-FID).[162] Such large-volume reaction chambers made of, or covered with, chemically inert material are used to minimize the possible effects of the reactor walls on the results. Ohta[163] used a 0.2-L quartz cell and GC monitoring for measurements of OH rate constants with a variety of alkenes. Results obtained in this small quartz reactor are in good agreement with those obtained in much larger (4×10^2 to 3×10^4 times larger) chambers.[82] In addition to the 140-L reactor mentioned previously, Wallington and co-workers[158] also used 0.3-L Pyrex reactor coupled to an FTIR spectrometer. DeMore and co-workers[164] have systematically studied OH reactions with potential CFC and Halon substitutes between room temperature and 370 K using FTIR detection coupled to a 200-cm^3 thermostated quartz cell. They have also used GC detection in such measurements.[165,166]

As mentioned previously, the range of OH concentrations that can be produced in the reactor determines the range of the rate constants that can be measured using a relative rate technique: the higher the OH concentrations, the lower the rate constants that can be measured. Typical OH concentrations in smog chamber experiments when NO_x-containing air is irradiated[157] are $(1-4) \times 10^6$ molecule/cm^3. Photolysis of premixed HONO−air mixtures produced $(1-5) \times 10^7$ molecule/cm^3, and photolysis of methyl nitrite−NO−air mixtures[151] generated $(2-3) \times 10^8$ molecule/cm^3. Photolysis of ozone in the presence of water yields up to $(0.11-10) \times 10^{10}$ molecule/cm^3 in the reactor.[161,167] Recently, Chen et al.[162] employed irradiation of an O_3-H_2O mixture with the continuous injection of ozone, thereby allowing them to decrease the initial O_3 concentration in the reactor and the associated OH loss via reaction with O_3.[162] They estimated the OH concentration to be (0.5 to 1.2) $\times 10^{11}$ molecule/cm^3. Thus, the characteristic concentrations of OH in relative rate experiments range from values that are comparable with those in the real atmosphere to about 5 orders of magnitude higher.

To illustrate the capability of the relative rate technique, we can consider a typical study in which at least 10% compound conversion occurs during an hour of irradiation, producing an average hydroxyl concentration in the reactor of $\overline{[OH]}$. The measured rate constant under such conditions can be estimated from the expression

$$k\overline{[OH]}3.6 \times 10^3 \text{ s} \geq 0.1$$

or

$$k \geq 3 \times 10^{-5}/\overline{[OH]}, \quad \text{cm}^3 \text{ molecule}^{-1} \text{ s}^{-1}$$

Thus, for $<3 \times 10^8$ molecule/cm^3 (the approximate concentration in large smog chambers), this results in $k > 10^{-13}$ cm^3 $molecule^{-1}$ s^{-1} (as given in ref 82), while for $\overline{[OH]} \approx 10^{11}$ molecule/cm^3, it corresponds to $k > 3 \times 10^{-16}$ cm^3 $molecule^{-1}$ s^{-1}. Of course, the actual lower limit of the OH reaction rate constant measurable with any particular experimental setup depends on the precision of the monitoring technique, the irradiation wavelength range, the photochemical properties of reactants, and the acceptable level of precision of the results.

The use of H_2O or other compounds of low volatility in the production of OH restricts the low-temperature limit of such measurements because of the low saturated vapor pressures. The problem becomes even more acute in the case of O_3-H_2O mixture photolysis, where the reactant concentration needs to be lower than that of H_2O to minimize reaction of $O(^1D)$ with RH. Using H_2 as the H donor instead of H_2O can solve the vapor pressure problem. In addition, the reaction between OH and H_2 causes fewer problems at low temperatures because of its smaller rate constant. Nevertheless, many relative rate studies have been limited to the measurement of relatively fast OH reactions ($k > 10^{-13}$ molecule/cm^3) near and above room temperature. While Hsu and DeMore[168,169] have studied a number of slow OH reactions with rate constants varying from 3×10^{-13} molecule/cm^3 to 2.5×10^{-16} molecule/cm^3, these measurements have been limited to near and above room temperature. A notable exception has been the study of OH reaction with propane performed between $T = 227$ K and $T = 428$ K,[166] although this reaction is relatively fast with $k(T) > 3 \times 10^{-13}$ molecule/cm^3. This study used 184.9-nm (Hg discharge lamp) photolysis of N_2O to generate $O(^1D)$, which was scavenged by H_2 to produce OH. Recently, Chen et al.[162] demonstrated an ability to study slow OH reactions at atmospheric temperatures using the photolysis of ozone/H_2O mixtures to produce OH. To increase the hydroxyl concentration in the reactor, they used low concentrations of ozone, thereby reducing OH background loss via its reaction with O_3. To maintain the O_3 concentration in the reactor, the ozone-containing mixture was continuously injected. Using this technique, they studied the reaction between OH and CHF_3 over the temperature range from 253 to 328 K and were able to determine the OH rate constants as small as 0.9×10^{-16} molecule/cm^3.

Finally, several relative rate studies have been performed by using nonphotolytic "dark" chemical sources of hydroxyl radicals. Heterogeneous OH formation in a H_2O_2/NO_2-containing mixture was

used by Campbell et al.,[170] whereas Barnes et al.[171] used the homogeneous thermal decomposition of HO_2-NO_2 in the presence of NO.

$$HO_2NO_2 \rightleftarrows HO_2 + NO_2$$

$$HO_2 + NO \rightarrow OH + NO_2$$

The gas reaction between O_3 and N_2H_4 was used by Tuazon et al.[172] to maintain a OH concentration of about 3×10^7 molecule/cm^3. Recently, Finlayson-Pitts et al.[173] found that the "dark" reaction in some ozone/hydrocarbon mixtures generates hydroxyl radical concentrations on the order of 10^8 molecule/cm^3, approximately 10^2 times less than that in their relative rate experiments utilizing photolytic production. No discernible differences could be seen in the rate constant ratios obtained using "dark" chemistry or photolysis as the source of OH radicals. Nonphotolytic generation of OH can be important in studying easily photolyzed compounds. Such experiments are also simpler in their experimental design.

As with any experimental technique, the validity of the results is dependent on the degree to which the various issues raised previously can be addressed. Numerous investigators have shown that, when properly conducted, the relative rate technique is a powerful kinetic tool that is highly complementary to absolute techniques for the accurate determination of OH reaction rate constants and of atmospheric lifetimes.

5.4. Absolute Rate Constant Measurements and Secondary Chemistry

Key to the validity of an absolute technique for the determination of a reaction rate constant is the assumption that the results can be univocally related to the particular chemical process of interest. Despite the many precautions that can be taken, the reaction system cannot always be simplified sufficiently to guarantee this. The experimental results can be affected by three types of complicating chemistry: (i) "secondary" reactions with radical products of the reaction under study; (ii) reactions with possible radical products of the reactant photolysis; and (iii) reactions with stable products that have accumulated in the reactor. These complications result in an overestimation of the rate constant because of additional OH removal.

Reactions of OH with products of the reaction under study can take place in both pulse and flow experiments. The product, R, from reaction (R3) is a free radical in nature and can undergo further rapid reaction with hydroxyl[174] to give additional products that can accumulate in the reactor. Thus, the experimentally measured OH decay can have contributions from its reaction with R or even with products of its chemical transformations. In the case where reaction with R occurs, the OH reactive decay can be described as

$$\frac{d[OH](t)}{dt} = -\{k_{RH}[RH] + k_R[R](t)\}[OH](t) \quad (47)$$

$[R](t)$ is a function of the initial concentration of hydroxyl radicals, and, therefore, in the case of pseudo-first-order conditions, $[R](t) < [OH]_0 \ll [RH]$. Thus, only very fast reactions between OH and R can contribute to the overall OH decay rate by making $k_R[R](t)$ comparable with $k_{OH}[RH]$. On the basis of the fact that k_R should have a very small temperature dependence, typical for rate constants of any very fast reaction,[148] the second summand in eq 47 is essentially the same at any temperature.

In the majority of experimental investigations, the data (pseudo-first-order decay rates, τ^{-1}) are usually obtained over the same range of $k_{RH}[RH]$, independent of how fast or slow the reaction or how high or low the temperature. It is quite reasonable to make measurements over a given range of τ^{-1} (rather than a range of [RH]) over which the measurements can be made most precisely using a particular instrumental setup. Therefore, the range of $k_R[R]/k_{RH}[RH]$ values can be expected to be roughly the same at different temperatures, the magnitude depending only on the values of $k_{RH}[RH]$ and the initial hydroxyl concentration used (i.e., experimental conditions) as well as on the rate constant of the secondary reaction k_R. Thus, to a first approximation, a secondary reaction involving a radical product from the primary reaction results in the same *relative* overestimation of the rate constant over the temperature range of study. This results mainly in an overestimation in the Arrhenius *A* factor rather than an error in the activation energy. To avoid such complications, $k_{RH}[RH] \gg k_R[OH]_0 > k_R[R]$ is required. This requirement is much more stringent than the pseudo-first-order condition of $[RH] \gg [OH]_0$ because of the difference in the rate constants k_{RH} and k_R. Hence, high-precision test experiments performed with different initial hydroxyl concentrations should be conducted to check for the possible effects of secondary reactions.

The use of pulsed irradiation to generate the initial OH concentration can also cause the photofragmentation of the reactant producing radicals, R_{ph}, that are reactive toward OH. In this case, the reactive OH decay is described as

$$\frac{d[OH](t)}{dt} = -\{k_{RH}[RH] + k_{ph}[R_{ph}]\}[OH](t) = -\{k_{RH}[RH] + k_{ph}[RH]\Phi\sigma_{RH}\}[OH](t) \quad (48)$$

where $\Phi\sigma_{RH}$ is the integrated coefficient of photodissociation of RH. The reaction rates of OH with both RH and photofragments R_{ph} are proportional to the RH concentration (in contrast with the case of secondary reactions discussed previously). Thus, reactions with photofragments result in the same *absolute* overestimation of the rate constant over the temperature range, and the slope of a plot of the observed rate constant, k_{RH}^{obs} versus flash energy, should be independent of the rate constant, k_{RH} (and, hence, of temperature). In this case, the relative overestimation of the rate constant can be more pronounced at low temperatures, resulting in an underestimation of the derived Arrhenius activation energy or even in curvature of the Arrhenius plot.

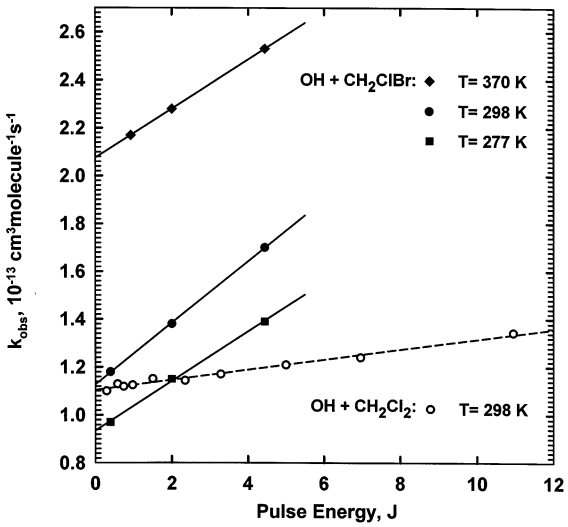

Figure 1. Dependence of the observed reaction rate constant (obtained in flash photolysis−RF experiments) for the reactions of OH with CH_2ClBr (at 277, 298, and 370 K)[175] and CH_2Cl_2 (at 298 K)[176] on the Xe lamp flash energy.

Figure 1 illustrates this example using the results of an FP−RF study of the OH reaction with CH_2ClBr at different temperatures and pulse energies of a Xe flash lamp.[175] The nearly constant slopes of the dependences obtained at different temperatures (different rate constant values) are indicative of the photofragmentation origin of complicating reactions. In the case of interference due to a secondary radical reaction (case 1), the slope should increase with increasing rate constant (or temperature). The dependence obtained for the OH reaction with CH_2Cl_2 is also shown.[176] The slope is about $^1/_6$ that observed for the OH + CH_2ClBr reaction despite the nearly identical value of the rate constant. This difference is consistent with much lower UV absorption of CH_2Cl_2, and the flash energy dependence can again be associated with reactions with photofragments.

Note that both radical products, R and R_{ph}, can also undergo further chemical reactions with the mixture components in the reactor generating more or less reactive products. The concentration of such products cannot exceed the initial OH concentration in the flow experiment. However, in a pulsed experiment, the multipulse irradiation of the mixture can result in the buildup of a higher concentration of products that can react with OH causing additional error in the measured rate constant. Such products can also diffuse to the reactor walls between flashes to undergo heterogeneous processes, releasing new compounds into the mixture. To avoid these complications, pulsed experiments are usually performed in a slow flow mode to replenish the irradiated mixture between flashes.

Test experiments performed with variation of the flash or laser intensity, the concentration of the OH photoprecursor (the initial OH concentration in the case of the flow technique), and the total flow rate are necessary to test for all of the previously mentioned complications. Demonstrating the absence of any complicating chemistry requires very precise kinetic measurements performed over a wide range of parameters. For example, a twofold change in any of these parameters can be used to check for the presence of large error due to such additional reactions. Nevertheless, a precision of the kinetic measurements of better than 5% is needed to check for the presence of a 10% contribution from complicating chemistry. Alteration of the photolysis wavelength and precursor in a pulsed experiment can be very helpful in proving the accuracy of the result. In general, any reduction of the photochemical impact on the system will result in reduced complications. However, decreasing the initial hydroxyl concentration, $[OH]_0$, can reduce the precision of the results as a result of the deterioration of signal-to-noise.

5.5. Reactive Impurities

The presence of reactive impurities in the sample of the compound to be studied is potentially the most serious problem encountered in an absolute rate technique and is especially difficult to diagnose for slow OH reactions. Contributions of impurity reactions to the measured OH decay rate cannot be revealed by the test experiments discussed previously. Their detection requires detailed sample analysis and purification. In the presence of small amounts of very reactive impurities in the RH sample, OH radicals will undergo reactions both with RH and with the impurity

$$\mathrm{OH} + \begin{cases} \mathrm{RH} \xrightarrow{k_{\mathrm{RH}}} \text{products} \\ \text{impurity} \xrightarrow{k_{\mathrm{imp}}} \text{products} \end{cases}$$

When only the change in [OH](t) is monitored, data reduction will result in a somewhat larger "effective" rate constant

$$k_{\mathrm{eff}} \cong k_{\mathrm{RH}} + \frac{[\mathrm{impurity}]}{[\mathrm{RH}]} k_{\mathrm{imp}} \qquad (49)$$

rather than k_{RH}. The OH reaction rate constant for some typical impurities can be as high as 10^{-10} cm^3 molecule^{-1} s^{-1} and even higher.[148] Such chemicals can be present as residual impurities from the compound's manufacture, intentionally added chemical stabilizers, or products of decomposition during storage. Numerous studies of the OH reactivity of halogenated hydrocarbons, which have been under consideration as CFC and Halon substitutes, have been compromised by the effects of such impurities. Unsaturated hydrohalocarbons are among the most common impurities. For example, the presence of 1,1-dichloroethene, $CH_2{=}CCl_2$ (whose OH rate constant is $k_{CH_2CCl_2}(T) = 1.9 \times 10^{-12} \exp\{+530/T\}$ cm^3 molecule^{-1} s^{-1}),[57] in samples of $CH_3{-}CFCl_2$ (a CFC replacement known as HCFC-141b) was a source of large errors in the early determinations of its OH rate constant and atmospheric lifetime.[17,177,178] The present recommendation for the rate constant of this reaction[57] is $k_{CH_3CFCl_2}(T) = 1.25 \times 10^{-12} \exp\{-1600/T\}$ cm^3 molecule^{-1} s^{-1}, which gives 5.8×10^{-15} cm^3 molecule^{-1} s^{-1} and 2.1×10^{-15} cm^3 molecule^{-1} s^{-1} at $T = 298$ K and $T = 250$ K, respectively.[179,180] Thus, the presence

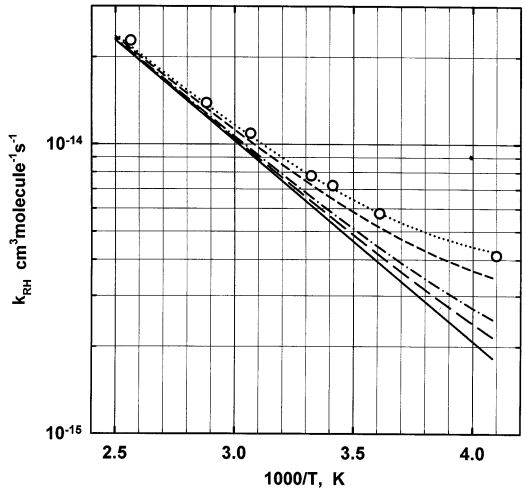

Figure 2. Calculated "effective" rate constants for the reaction between OH and CH_3CFCl_2 contaminated with 0% (solid line), 0.002% (long dashed line), 0.004% (dashed−dotted line), and 0.01% (short dashed line) $CH_2{=}CCl_2$. The dotted line (corresponding to 0.0148% $CH_2{=}CCl_2$) is a fit to the experimental data[178] shown as circles.

of an amount of $CH_2{=}CCl_2$ as small as 0.01% in a sample of HCFC-141b would result in about 20% overestimation of its OH reaction rate constant at $T = 298$ K and about 80% at $T = 250$ K! This impurity would also cause a noticeable upward curvature of the Arrhenius plot, as was observed in the earlier studies of the reaction.[178] In general, such a curvature can be indicative of the presence of reactive impurities. However, it can be statistically distinguishable only when the contribution from the reaction with impurities is high enough. With impurity errors on the order of 10−20%, curvature may not be readily recognized and underestimated Arrhenius parameters (A and E/R) will be obtained. Figure 2 illustrates this example, showing the present recommendation of $k_{CH_3CFCl_2}(T)$ and the calculated "effective" OH rate constant when a $CH_2{=}CCl_2$ impurity is present in the amounts of 0.002, 0.004, 0.01, and 0.0148% respectively between 245 and 400 K. (The last impurity amount was obtained from the best fit to one of the earlier experimental data sets on this reaction.)[178] Such impurity levels result in overestimations of $k_{CH_3CFCl_2}(T)$ at the lowest temperature of 18, 36, 91, and 135%. The presence of the same chemical, $CH_2{=}CCl_2$, as a decomposition product of MCF was a potential reason for early overestimations of the rate constant for the reaction between OH and CH_3CCl_3.

Reactive impurities and, especially, added stabilizers can also pose a problem when relatively fast reactions are under study. The OH rate constant of tetrafluoroethene, $CF_2{=}CF_2$, is approximately 1.0×10^{-11} cm^3 molecule^{-1} s^{-1} at room temperature.[57] However, because of its tendency to polymerize, about 1% of α-terpinene or α-pinene is used as a stabilizer. As any chemicals used for radical scavenging during storage, they are very reactive themselves (having OH rate constants of ca. 3×10^{-10} cm^3 molecule^{-1} s^{-1} and 5×10^{-11} cm^3 molecule^{-1} s^{-1}, respectively).[82,181] This could cause an overestimation of about 30 and 5%, respectively, if no purification was performed before conducting $k_{C_2F_4}$ measurements.[182]

Significant attention must be paid to purity analysis and impurity identification when compounds of low reactivity are under study. GC, GC-FID, GC-MS, FTIR, and UV absorption analytical techniques are widely used for this purpose. Absorption in the vacuum UV was found to be a very sensitive method to detect parts per million levels of unsaturated micro-impurities in samples of nonabsorbing compounds such as alkanes and fluoroalkanes.[147,182] The use of samples from different manufacturers or different production lots, coupled with additional purification,[147,176,182−185] can be important in avoiding errors due to the presence of nonrecognized or undetected reactive micro-impurities in samples of chemicals that react slowly with OH, like many of CFC and Halon candidate substitutes.

5.6. Data Accuracy and Presentation

The proper derivation and clear presentation of a OH rate constant and its uncertainties are important elements for enabling data evaluation and the subsequent use of the data in atmospheric applications with confidence in their accuracy. The evaluation of experimental errors has been discussed in many publications, some of which have specifically treated error analysis in gas-phase rate constant measurements.[79,80,186−191]

The uncertainty in a measured rate constant can arise from three different sources: (a) random fluctuations of the detection system signal that result in a statistical uncertainty associated with the data treatment; (b) fluctuations (or reproducibility) of the measured parameters of the kinetic experiment that result in an instrumental uncertainty; and (c) systematic errors, which are not caused by a fluctuation of any measured value but rather arise from biases in the absolute calibrations of the measuring tools or from a possible unaccounted chemical or physical process.

Strictly speaking, only the first source can generate "normally" distributed values, attaining a Gaussian distribution in repeated observations. For example, in the case of photon counting in a RF or LIF technique, the count rate distribution can be easily tested by comparing the mean count rate with its standard deviation to ensure the proper operation of the detection system. Under such circumstances, standard statistical methods are adequate for treating the signals for deriving the kinetic parameters and their statistical uncertainties. Other parameters required for calculating the OH rate constant are usually obtained from instrumental measurements using calibrations with specific uncertainties. The distribution of these values is again assumed to be "normal", and, thus, standard statistical methods have generally been used for their analysis.

The parameter characterizing the uncertainty of the mean value obtained from the statistical analysis of normally distributed data is the "standard error" or "standard deviation of the mean". It is often

mistakenly referred to as the "standard deviation", which is a different statistical parameter characterizing the data scattering (i.e., the width of the Gaussian distribution, not the uncertainty of the derived mean value). In the case of a normal distribution of measured values, there are probabilities of about 68 and 95% that the derived mean value is within 1 and 2 standard errors, respectively, from the true value, provided that the number of repetitive measurements is sufficiently large. In the more common case of a restricted number of measurements, the standard error should be multiplied by the student's coefficient associated with the actual number of measurements.

The uncertainty in the rate constant obtained from the statistical treatment of the signal and data fitting (the first source of uncertainty) represents the data reproducibility, that is, the precision of the measurements. The cumulative error due to statistical uncertainties in measured experimental parameters (the second source of the uncertainty) represents part of the instrumental uncertainty. In the absence of systematic errors, the combination of these uncertainties represents the accuracy of the obtained rate constant.

Systematic errors are the most difficult to quantify because there are often no general approaches for examining their possible sources and they are nonstatistical. Some systematic uncertainties are instrumental in nature. Diffusion processes in the laminar flow technique, the flow velocity radial profile in the turbulent flow technique, and temperature measurements of gas mixtures are but a few examples. Other systematic uncertainties are chemical in nature, such as those associated with complicating chemistry, reactant photolysis or decomposition, or sample contamination (as discussed previously). All of these uncertainties usually result in an absolute bias in the derived rate constant rather than a range of statistical uncertainties. The proper reporting of all estimated uncertainties is extremely important for data evaluation in which the results from various determinations are compared to make recommendations for the users.

The uncertainty of k_{RH} due to accumulation of the uncertainties of all noncorrelated measured parameters described as type "b" may be estimated from the theory of propagation of errors

$$(\Delta k_{RH}^{instr})^2 = \sum_i \left(\frac{\partial k_{RH}(M_i)}{\partial M_i} \Delta M_i \right)^2 \qquad (50)$$

where the M_i's are the measured parameters upon which the rate constant k_{RH} depends, that is, $k_{RH} = k_{RH}(M_i)$. In the case of an absolute technique, the temporal profile of the OH concentration is the primary source of the kinetic information, whereas the gas flow rates (F_i), pressure (P), and temperature (T) are the main gas dynamic parameters used in the k_{RH} calculations. Additional parameters, such as reactant dilution in the storage volume or the reactant concentration when measured directly in the flow, can also be involved.

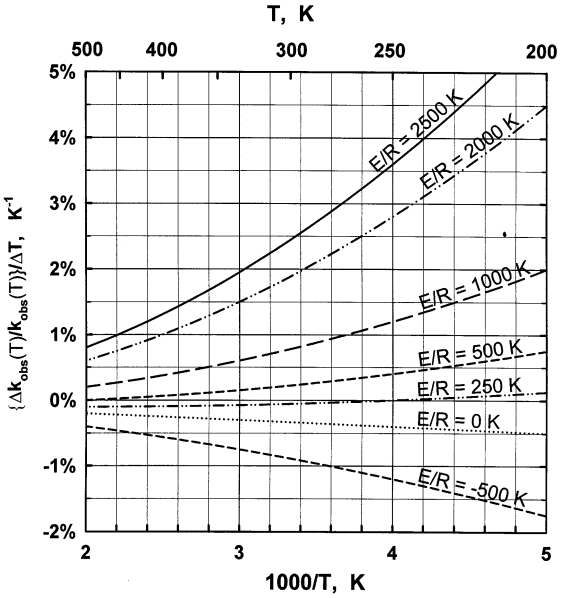

Figure 3. Relative error in the rate constant, arising from a 1 K error in the measurement of the temperature of the reacting mixture, shown for different E/R Arrhenius parameters.

It is worthwhile to take a closer look at the contribution from uncertainties in the reactor temperature. This can be estimated from expression 28 for the determination of k_{RH} from the experimental data as

$$\frac{\partial k_{RH}(T)}{\partial T} = \frac{\partial}{\partial T} \frac{\partial^2 \ln\{[OH]_0/[OH]\}}{\partial t\, \partial[RH]} = \frac{\partial}{\partial[RH]} \frac{\partial}{\partial T} \frac{\partial \ln\{[OH]_0/[OH]\}}{\partial t} = \frac{k_{RH}(T)}{T}\left(\frac{E}{RT} - 1\right) \qquad (51)$$

and, therefore, the relative error in the rate constant due to an uncertainty in the gas temperature, ΔT, is given by

$$\frac{\Delta k_{RH}(T)}{k_{RH}(T)} = \left(\frac{E}{RT} - 1\right)\frac{\Delta T}{T} \qquad (52)$$

Figure 3 shows the relative error in k_{obs} due to a 1 K error in the measurement of the gas temperature for a range of the Arrhenius E/R parameter.[148] One can see that such errors become more important at low temperatures where even a 1 K uncertainty in the temperature can cause a few percent uncertainty in the rate constant, making this a serious source of instrumental error at temperatures of atmospheric interest. However, for fast OH reactions, characterized by E/R values between 0 and 400 K, much smaller errors occur.

On the basis of uncertainties in other experimental parameters such as the measured flow rate of the ith gas flowing through the reactor (F_i), the pressure (P), and the temperature (T), the propagated instrumental uncertainty for the determination of k_{RH} can be estimated for a particular experimental tech-

nique. In the case of a pulsed experiment, one can derive

$$\left(\frac{\Delta k_{RH}^{inst}}{k_{RH}}\right)^2_{pulse} = \frac{\sum_i \Delta F_i^{\,2}}{(\sum_i F_i)^2} + \frac{\Delta F_{RH}^{\,2}}{F_{RH}^{\,2}} - \frac{2\Delta F_{RH}^{\,2}}{F_{RH}\sum_i F_i} + \frac{\Delta P^2}{P^2} + \left(\frac{E}{RT} - 1\right)^2 \frac{\Delta T^2}{T^2} \quad (53)$$

where we have assumed that the time interval is known absolutely and does not introduce any additional uncertainty. Given typical uncertainties in these parameters, the relative instrumental uncertainty in k_{RH} can be on the order of 4% in a pulsed experiment.[185] In the case of independent measurements of the reactant concentration in the total gas flow, the first four summands in eq 53 are replaced with the cumulative uncertainty of that determination, $(\Delta[RH]/[RH])^2$. Such measurements can result in a larger statistical uncertainty of k_{RH}, but they decrease the possibility of systematic errors due to reactant absorption or decomposition in the gas-handling system. In the case of a laminar flow experiment, the reaction time interval is implicitly associated with measurements of both the distance interval (z) and the absolute value of the flow velocity, and the corresponding expression becomes

$$\left(\frac{\Delta k_{RH}^{inst}}{k_{RH}}\right)^2_{flow} = \frac{4\sum_i \Delta F_i^{\,2}}{(\sum_i F_i)^2} + \frac{\Delta F_{RH}^{\,2}}{F_{RH}^{\,2}} - \frac{4\Delta F_{RH}^{\,2}}{F_{RH}\sum_i F_i} + \frac{\Delta P^2}{P^2} + \frac{\Delta z^2}{z^2} + \left(\frac{E}{RT} - 1\right)^2 \frac{\Delta T^2}{T^2} \quad (54)$$

These additional terms result in a typical relative instrumental uncertainty in k_{RH} for a flow experiment slightly larger than that in the pulsed experiment.

An analytical expression relating the temperature dependence of the derived rate constant is useful in several ways. First, it is a convenient representation of the rate constant at any temperature over the measured range. Second, it can be used to extrapolate a value for k_{RH} beyond the temperature range over which the experiments were performed, provided the expression does indeed represent the dependence over an extended temperature range. This will be discussed further in the next section. Third, the parameters associated with such an analytical expression may be used together with theoretical calculations to get an insight into the mechanism of the elementary reaction. A statistical treatment is generally applied in fitting the desired analytical expression to the available experimental data set.

The Arrhenius expression is most commonly used as an empirical representation of the temperature dependence of a rate constant, with the best A and E/R parameters determined from a standard least-squares analysis:

$$k_{RH}(T) = A \exp\{-E_{RH}/RT\} \quad (55)$$

A proper statistical weighting is very important in this procedure, especially because the measured values of k_{RH} can be very different at different temperatures and the Arrhenius dependence is not linear. From a purely statistical point of view, the rate constants should be weighted by the reciprocal of the squares of their standard errors, $w_i = 1/\sigma_i^2$. However, on the basis of the analysis of a kinetic experiment given in the discussion of secondary chemistry, the relative error in a measured rate constant is generally temperature-independent, unless some systematic errors appear at the extreme ends of the temperature range. On the other hand, the statistically derived error of k_{RH} often does not comply with a normal distribution hypothesis. Hence, an alternative weighting of $w_i = 1/k_i^2$ is often applied when the same relative errors are ascribed to all individual rate constants in the least-squares analysis. This weighting is usually preferred when evaluating reaction rate constants simply because it has general applicability because statistical standard errors are not always available from the original papers and can be affected by nonstatistical factors that are difficult to account for. In the real case, the Arrhenius parameters derived using either statistical weights should be (and generally are) about the same within the error of the fit. Any serious disagreement is an indication of poor measurement precision.

Another approach in deriving the temperature-dependence parameters is the use of the logarithmic form of the Arrhenius equation

$$\ln(k_{RH}) = \ln A - E_{RH}/RT \quad (56)$$

which relies on the linear dependence of $\ln(k_{RH})$ on $1/T$. This approach simplifies the determination of A and E/R as the intercept and the slope, respectively, of a linear least-squares analysis. The use of eq 56 for the least-squares analysis with $w_i = 1$ is roughly equivalent to the use of eq 55 with $w_i = 1/k_i^2$. Table 1 illustrates these points with Arrhenius parameters derived from the fit of the data obtained for the reaction between OH and CH_3CF_3 by three different research groups using four experimental techniques. The top line in each data set (bold) shows results obtained using eq 55 with $w_i = 1/k_i^2$; the second line (italics) shows the results of a fit to the same data set using eq 56 with $w_i = 1$; and the third line shows the results obtained using eq 55 with $w_i = 1/\sigma_i^2$ with standard errors (σ_i) from the original absolute technique determinations.

An increasing number of precise determinations of OH rate constants performed over a wide temperature range indicate real curvature in an Arrhenius plot of $\ln(k)$ versus $1/T$. Hence, a modified Arrhenius expression is commonly used to present the temperature dependence of the rate constant in such cases

$$k_{RH}(T) = A\left(\frac{T}{298\ \mathrm{K}}\right)^n \exp\{-E_{RH}/RT\} \quad (57)$$

Table 1. Arrhenius Parameters Determined for the Reaction between OH and CH_3CF_3 (HFC-143a)[a,b]

technique	temperature range, K	$k_{HFC-143a}(298) \times 10^{15}$, cm^3 $molecule^{-1}$ s^{-1}	E/R, K	$A \times 10^{12}$, cm^3 $molecle^{-1}$ s^{-1}
DF-LMR[180]	261−334	**1.45 ± 0.027**	**2004 ± 46.6**	**1.21 ± 0.18**
		1.46 ± 0.028	*2000 ± 46.9*	$1.20^{+0.19}_{-0.17}$
		1.41 ± 0.021	2088 ± 37.4	1.56 ± 0.18
FP-LIF[180]	266−374	**1.169 ± 0.0073**	**2010 ± 18.6**	**0.994 ± 0.066**
		1.172 ± 0.0074	*2010 ± 18.5*	$0.991^{+0.067}_{-0.063}$
		1.170 ± 0.0062	2009 ± 19.1	0.990 ± 0.065
relative CH_4[168]	298−403	**1.27 ± 0.056**	**2000 ± 93.5**	**1.04 ± 0.3**
		1.28 ± 0.056	*1998 ± 89.8*	$1.04^{+0.32}_{-0.25}$
relative CHF_2CF_3[168]	298−383	**1.25 ± 0.012**	**2070 ± 22.5**	**1.30 ± 0.084**
		1.245 ± 0.011	*2070 ± 21.4*	$1.30^{+0.087}_{-0.081}$
FP-RF[62]	298−370	**1.254 ± 0.030**	**1965 ± 57.3**	**0.92 ± 0.16**
		1.257 ± 0.031	*1965 ± 58.7*	$0.915^{+0.177}_{-0.149}$
		1.246 ± 0.0187	2012 ± 56	1.07 ± 0.19

[a] The results of the standard nonlinear fit using eq 55 with statistical weights $w_i = 1/k_i^2$ are in bold; the results of a linear fit using eq 56 are in italics; and the results of the standard nonlinear fit using the statistical standard errors of individual measurements (σ_i) reported in the original papers for statistical weighting $w_i = 1/\sigma_i^2$ are shown as normal text. [b] Uncertainties are one standard error from a corresponding fit to the published data.

Such a three-parameter fit is generally far less sensitive to the actual values of the parameters. Nevertheless, when applied to a precise data set obtained over a very wide temperature range, it can yield parameters with quite low statistical errors.[184,185] However, application to a subset of the same data over any portion of the temperature range usually results in different parameters with higher statistical errors. Therefore, the statistical standard error of A, n, and E/R is not a measure of the quality of the fit or of the data scattering. The standard deviation (or even the average deviation) of the data set is more appropriate for quantifying the data scattering around the best-fitted dependence. The previous discussion on data fitting applies to this case as well, where A, n, and E/R should be considered purely as algebraic parameters of the fit rather than ascribed to something that can be compared with the theory.

5.7. Evaluation of OH Reaction Rate Constant Data

The purpose of data evaluation is to provide the user community with the most reliable rate constants based on a critical analysis of all available information. This includes a comparison of the data obtained by different research groups using different techniques and different reactant samples to estimate rate constant uncertainties not necessarily recognized in the original studies. This process should actually be an intrinsic component in the reporting of any rate constant remeasurements. For example, the authors of ref 192 were able to explain nearly a 30% overestimation of the rate constant previously recommended for the reaction between OH and CH_4 as due to secondary chemistry associated with the high OH concentrations used in earlier studies.

On the other hand, when appropriate care has been taken to minimize the effects of impurities or complicating chemistry in well-characterized laboratory experiments, excellent agreement among the results obtained in different laboratories using different techniques can be achieved. A good example of this is the reaction between OH and propane, for which the measured rate constants from four independent absolute studies agree within about 5% between 400 and 200 K (see ref 184 for a complete discussion). In this case, the reported overall uncertainties of the individual determinations may actually be too conservative. Nevertheless, the task of providing a recommended rate constant expression may not always be straightforward. Difficulties can still arise from small residual systematic errors in data sets spanning slightly different temperature ranges and from the existence of real Arrhenius curvature in the rate constant, not evident from data sets obtained over a limited temperature range. Two examples will be given to illustrate these issues.

For the reaction of OH with CH_3CF_3 (HFC-143a), the results from several studies can be analyzed individually to give Arrhenius temperature dependences (E/R) of 2004,[180] 2010,[180] 2000,[168] 2070,[168] and 1965 K,[62] as shown in Table 1. Thus, these five different studies yield data sets that are in very good agreement and are essentially parallel on an Arrhenius plot, differing only in their Arrhenius preexponential factors. This is probably an indication of small systematic errors rather than just data scattering. As a result of the slight differences in the temperature regions covered by each study, a combined fit of the composite data set introduces a systematic bias into the derived temperature dependence and yields an Arrhenius activation energy of nearly 2200 K, significantly higher than that obtained in any single investigation.[193] The use of such a composite fit results in an underestimation of the rate constant at lower temperatures. Thus, while it may be appropriate in many cases to conduct a fit to a combined data set, one must be conscious of the potential for the introduction of a systematic bias. In such cases, it may be more appropriate to focus on a room temperature rate constant recommendation and to use an average of the various measured temperature dependences (as has been done for this reaction in the latest NASA Data Panel recommendation).[57]

It has been well-documented that real Arrhenius curvature around and below room temperature exists

for the reactions of OH with many compounds. Such low-temperature curvature has been observed for OH reactions with unsaturated organics[194] as well as with carbonyl compounds.[195−199] In such cases, the nonlinear Arrhenius dependence has been associated with intermediate adduct formation.[200] The curvature can also be the result of the existence of different reaction channels (abstraction of an H atom from different sites),[114,184] tunneling at lower temperatures, or the existence of reactant conformers in a seemingly symmetric molecule whose populations and reactivities differ with temperature. Such curvature can make it appear that there is a significant disagreement between two studies conducted over different temperature ranges. This can be illustrated using the database for the reaction between OH and CH_3CHF_2 (HFC-152a). Until recently, the most extensive studies of the temperature dependence of this reaction appeared to be in significant disagreement. The results of a relative rate investigation,[168] conducted at room temperature and above, yielded a temperature dependence considerably stronger than that derived from an absolute rate study[201] using data obtained at room temperature and below. These apparent differences have led to uncertainties in the calculation of the tropospheric lifetime of HFC-152a. A more recent study[185] conducted over a broader temperature range than the combined range of these two earlier studies clearly demonstrated Arrhenius curvature and agrees with these earlier results not only in the rate constant values but also in the temperature dependence derived over different temperature regions. Thus, the new rate constant recommendation for use in atmospheric studies has been derived from a fit to the predominantly lower temperature data. This fit, however, is not applicable for use as a reference expression in normalizing relative rate data obtained at room temperature and above. As in the first case described, if care is not taken in examining the complete database to understand the source of possible differences, systematic biases can be introduced into the recommendations made for use in atmospheric lifetime estimations.

Fortunately, however, as discussed earlier for eq 17, the appropriate scaling temperature for estimating the lifetimes (associated with removal by tropospheric OH) of most reactive trace gases is 272 K. This temperature is sufficiently close to room temperature so that the appropriate rate constant can often be derived from a short extrapolation of data obtained at room temperature and above without introducing a large systematic bias. Nevertheless, rate constants over the full range of atmospheric temperatures are needed for the complete modeling of a compound's distribution throughout the atmosphere, up to the top of the tropopause (which is the important region for global warming effects) and in the stratosphere (where halogen atoms can be released to participate in ozone-destroying reactions).

A number of semiempirical approaches have been developed for predicting and estimating reaction rate constants on the basis of molecule properties such as bond dissociation energies, ionization energies, infrared frequencies, and so forth (see ref 202). Two methods in particular have utilized the available evaluated data on OH reactivity in their development. Atkinson[203] has developed an empirical estimation procedure that is based on the correlation between the OH reactivity toward both saturated and unsaturated compounds and their molecular structure. Its predictive accuracy of OH reaction rate constants for both abstraction and addition reactions is within a factor of 2 of the experimental values in about 90% of the 485 tested organic compounds.[202] The technique is periodically tested and updated.[202,204,205] While giving reasonably reliable estimates within the database used for its development, the technique lacks assurance in its reliability when extrapolated to organic compounds outside that database. Unfortunately, the most common and serious disagreements between the estimated and measured OH reaction rate constants occur for partially halogenated organic compounds, which often are of particular environmental interest, as discussed earlier. DeMore[206] developed a similar procedure specifically focused on estimating the rate constants of OH reactions with partially halogenated alkanes using multiplicative factors for various substituent groups. This algorithm yields the rate constants within the database used in its formulation to within a factor of 1.35 and exhibited similar predictive accuracy for several test reactions.[165,206] Because this technique was focused entirely on haloalkanes, the improved predictive capability for this class of compounds is not surprising.

Ab initio calculations of molecular parameters combined with transition state theory have gained wide use as "purely theoretical" methods of computing reaction rate constants. Present levels of computing allow very accurate ab initio calculations of the structure of an individual molecule using reasonably large basis sets, even in the case of multielectron molecular systems containing halogen (Cl, Br) atoms. Much less confidence, however, exists in the estimation of the parameters of the reaction transition state and of possible corrections for nonadiabatic pathways (tunneling corrections). As a result, improvements in and sophistication of calculations of the reaction transition state and potential barrier do not necessary yield more realistic results. There are unfortunately no absolute criteria by which to judge the improvement of quality of such estimations. At higher temperatures, the calculated parameters of the potential barrier and transition state can be adjusted to fit to the available experimental data. This model with adjusted parameters can then be used to calculate the rate constants above the temperature interval of the measurements with some confidence. At the low temperatures of atmospheric interest, the situation is more uncertain because of tunneling corrections, which can be very important for H abstraction reactions. Again, the correct shape of the calculated potential barrier is of crucial importance. Our calculations of the OH reaction rate constant with halogenated methanes can illustrate this point.[207−209] Ab initio calculations for the reaction between OH and CH_2Br_2 were performed at different levels of theory using different methods for estimat-

ing the tunneling correction. It was found that the most computationally demanding method using the largest basis set does not necessarily give the best fit to the available data; the choice of the best tunneling correction was also not obvious. Nevertheless, the empirically determined best calculational approach did a reasonably good job in predicting the rate constants for the OH reactions with other halogenated methanes. Calculations of complex reacting systems at the highest levels of theory can be as time and labor consuming as the experimental study of the reaction itself yet give no assurance in the accuracy of the calculated rate constant for an unmeasured reaction. Thus, the ab initio−transition state theory method requires high quality experimental data for its further development. Nevertheless, it can be used for semiempirical extrapolation of measured data toward higher temperatures and to understand and possibly predict reaction pathways.

6. Summary

It is quite clear that the concept of an atmospheric lifetime (with the appropriate caveats discussed previously) has proved useful in considering the environmental effects of a variety of naturally occurring and anthropogenically produced chemicals. Advances in laboratory techniques have provided the capabilities for determining reaction rate constants of sufficient accuracy for use in estimating such lifetimes via a variety of calculational techniques. Nevertheless, potential pitfalls in both the laboratory and modeling arenas require careful attention and analysis to ensure that sound fundamental bases are provided for future technology and policy decisions.

7. References

(1) Levy, H. *Science* **1971**, *173*, 500.
(2) *Scientific Assessment of Ozone Depletion: 2002*; Report No. 47; Global Ozone Research and Monitoring Project, World Meteorological Organization: Geneva, 2003.
(3) *Climate Change 2001: The Scientific Basis*; Contribution of Working Group I to the Third Assessment Report of the Intergovernmental Panel on Climate Change; Cambridge University Press: New York, 2001.
(4) Haagen-Smit, A. J. *Ind. Eng. Chem.* **1952**, *44*, 1342.
(5) (a) Crutzen, P. J. *Pure Appl. Geophys.* **1973**, *106*−*108*, 1385. (b) Crutzen, P. J. *Tellus* **1974**, *16*, 47.
(6) Chameides, W. L.; Walker, J. C. G. *J. Geophys. Res.* **1973**, *78*, 8751.
(7) Thompson, A. M. *Science* **1992**, *256*, 1157.
(8) Atkinson, R. *Atmos. Environ.* **2000**, *34*, 2063.
(9) Yin, F.; Grosjean, D.; Seinfeld, J. *J. Atmos. Chem.* **1990**, *11*, 309.
(10) Kiehl, J.; Schneider, T.; Rasch, P.; Barth, M.; Wong, J. *J. Geophys. Res.* **2000**, *105*, 1441.
(11) Bolin, B.; Rodhe, H. *Tellus* **1973**, *25*, 58.
(12) Prather, M. J. *Geophys. Res. Lett.* **1996**, *23*, 2597.
(13) Prather, M. J. *Global Biogeochem. Cycles* **1997**, *11*, 393.
(14) Ko, M. K. W.; Sze, N.-D.; Scott, C. J.; Weisenstein, D. K. *J. Geophys. Res.* **1997**, *102*, 25507.
(15) *Climate Change 1995: The Science of Climate Change*; Contribution of Working Group I to the Second Assessment Report of the Intergovernmental Panel on Climate Change; Cambridge University Press: New York, 1996; Vol. 65.
(16) Volk, C. M.; Elkins, J. W.; Fahey, D. W.; Dutton, G. S.; Gilligan, J. M.; Loewenstein, M.; Podolske, J. R.; Chan, K. R.; Gunson, M. R. *J. Geophys. Res.* **1997**, *102*, 25543.
(17) Ravishankara, A. R.; Lovejoy, E. R. *J. Chem. Soc., Faraday Trans.* **1994**, *90* (15), 2159.
(18) Prather, M. J. *Geophys. Res. Lett.* **1994**, *21*, 801.
(19) Prather, M.; Derwent, R.; Ehalt, D.; Fraser, P.; Sanhueza, E.; Zhou, X. Other Tracer Gases and Atmospheric Chemistry. *Climate Change 1994*; Cambridge University Press: New York, 1995, Vol. 73.
(20) Schimel, D.; Alves, D.; Enting, I.; Heimann, H.; Joos, F.; Raynaud, D.; Wigley, T.; Prather, M.; Derwent, D.; Ehalt, D.; Fraser, P.; Sanhueza, E.; Zhou, X.; Jonas, P.; Charlson, R.; Rodhe, H.; Sadasivan, S.; Shine, K. P.; Fouquart, Y.; Ramaswamy, V.; Solomon, S.; Srinivasan, J.; Albritton, D.; Isaksen, I.; Lal, M.; Wuebbles, D. Radiative Forcing of Climate Change. *Climate Change 1995: The Science of Climate Change*; Contribution of Working Group I to the Second Assessment Report of the Intergovernmental Panel on Climate Change; Cambridge University Press: New York, 1996; Vol. 65.
(21) Kanakidou, M.; Dentener, F. J.; Crutzen, P. J. *J. Geophys, Res.* **1995**, *100*, 18781.
(22) Wine, P. W.; Chameides, W. L. *Scientific Assessment of Stratospheric Ozone: 1989*; Report No. 20; Global Ozone Research and Monitoring Project, World Meteorological Organization: Geneva, 1989; Vol. II, p 273.
(23) Prather, M. J. *Science* **1998**, *279*, 1339.
(24) Khalil, M. A. K. In *The Handbook of Environmental Chemistry*; Fabian, P., Singh, O. N., Eds.; Springer-Verlag: New York, 1998; Vol. 4, Part E, Chapter 2, p 45.
(25) Khalil, M. A. K.; Moore, R. M.; Harper, D. B.; Lobert, J. M.; Erickson, D. J.; Koropalov, V.; Sturges, W. T.; Keene, W. C. *J. Geophys, Res.* **1999**, *104*, 8333.
(26) Prentice, I. C.; Farquhar, G. D.; Fasham, M. J. R.; Goulden, M. L.; Heimann, M.; Jaramillo, V. J.; Kheshgi, H. S.; Le Quéré, C.; Scholes, R. J.; Wallace, D. W. R. The Carbon Cycle and Atmospheric Carbon Dioxide. *Climate Change 2001: The Scientific Basis*; Contribution of Working Group I to the Third Assessment Report of the Intergovernmental Panel on Climate Change; Cambridge University Press: New York, 2001; Vol. 183.
(27) Ehalt, D. H.; Dorn, H. P.; Poppe, D. *Proc. R. Soc. Edinburgh* **1991**, *97B*, 17.
(28) Graedel, T. E. *Chemical Compounds in the Atmosphere*; Academic Press: New York, 1978.
(29) Donahue, N.; Prinn, R. *J. Geophys. Res.* **1990**, *95*, 18387.
(30) Brune, W. *IGACtivities Newsletter* **2000**, *21*, 1.
(31) (a) Stimpfle, R. M.; Anderson, J. G. *Geophys. Res. Lett.* **1988**, *15*, 1503. (b) Stimpfle, R. M.; Lapson, L. B.; Wennberg, P. O.; Anderson, J. G. *Geophys. Res. Lett.* **1989**, *16*, 1433. (c) Stimpfle, R. M.; Wennberg, P. O.; Lapson, L. B.; Anderson, J. G. *Geophys. Res. Lett.* **1990**, *17*, 1905.
(32) (a) Carli, B.; Park, J. H. *J. Geophys. Res.* **1988**, *93*, 3851. (b) Carli, B.; Carlotti, M.; Dinelli, B.; Mencaraglia, F.; Park, J. H. *J. Geophys. Res.* **1989**, *94*, 11049.
(33) Jucks, K. W.; Johnson, D. G.; Chance, K. V.; Traub, W. A.; Margitan, J. J.; Osterman, G. B.; Salawitch, R. J.; Sasano, Y. *Geophys. Res. Lett.* **1998**, *25*, 3935.
(34) Pickett, H. M.; Peterson, D. B. *J. Geophys. Res.* **1993**, *98*, 20507.
(35) (a) Wennberg, P. O.; Stimpfle, R. M.; Weinstock, E. M.; Dessler, A. E.; Lloyd, S. A.; Lapson, L. B.; Schwab, J. J.; Anderson, J. G. *Geophys. Res. Lett.* **1990**, *17*, 1909. (b) Wennberg, P. O.; Cohen, R. C.; Stimpfle, R. M.; Koplow, J. P.; Anderson, J. G.; Salawitch, R. J.; Fahey, D. W.; Woodbridge, E. L.; Keim, E. R.; Gao, R. S.; Webster, C. R.; May, R. D.; Toohey, D. W.; Avallone, L. M.; Proffitt, M. H.; Loewenstein, M.; Podolske, J. R.; Chan, K. R.; Wofsy, S. C. *Science* **1994**, *266*, 398. (c) Wennberg, P. O.; Hanisco, T. F.; Cohen, R. F.; Stimpfle, R. M.; Lapson, L. B.; Anderson, J. G. *J. Atmos. Sci.* **1995**, *52*, 3413.
(36) Chance, K. V.; Traub, W. A.; Johnson, D. G.; Jucks, K. W.; Ciarpallini, P.; Stachnik, R. A.; Salawitch, R. J.; Michelsen, H. A. *J. Geophys. Res.* **1996**, *101*, 9031.
(37) Pickett, H. M.; Peterson, D. B. *J. Geophys. Res.* **1996**, *101*, 16789.
(38) Dorn, H.-P.; Hofzumahaus, A. *IGACtivities Newsletter* **2000**, *21*, 1 and references therein.
(39) Frost, G. J.; Trainer, M.; Mauldin, R. L.; Eisele, F. L.; Prevot, A. S. H.; Flocke, S. J.; Madronich, S.; Kok, G.; Schillawski, R. D.; Baumgardner, D.; Clarke, A.; Bradshaw, J. *J. Geophys. Res.* **1999**, *104*, 16041.
(40) Jaeglé, L.; Jacob, D. J.; Wennberg, P. O.; Spivakovsky, C. M.; Hanisco, T. F.; Lanzendorf, E. L.; Hintsa, E. J.; Fahey, D. W.; Keim, E. R.; Proffitt, M. H.; Atlas, E.; Flocke, F.; Schauffler, S.; McElroy, C. T.; Midwinter, C.; Pfister, L.; Wilson, J. C. *Geophys. Res. Lett.* **1997**, *24*, 3181.
(41) Prather, M. J.; Jacob, D. J. *Geophys. Res. Lett.* **1997**, *24*, 3189.
(42) Jaeglé, L.; Jacob, D. J.; Brune, W. H.; Wennberg, P. O. *Atmos. Environ.* **2001**, *35*, 469.
(43) Thompson, A. M. *Isr. J. Chem.* **1994**, *34*, 277.
(44) (a) Spivakovsky, C. M.; Yevich, R.; Logan, J. A.; Wofsy, S. C.; McElroy, M. B.; Prather, M. J. *J. Geophys. Res.* **1990**, *95*, 18441. (b) Prather, M. J.; Spivakovsky, C. M. *J. Geophys, Res.* **1990**, *95*, 18723. (c) Spivakovsky, C. M.; Logan, J. A.; Montzka, S. A.; Balkanski, Y. J.; Foreman-Fowler, M.; Jones, D. B. A.; Horowitz, L. W.; Fusco, A. C.; Brenninkmeijer, C. A. M.; Prather, M. J.; Wofsy, S. C.; McElroy, M. B. *J. Geophys. Res.* **2000**, *105*, 8931 and references therein.
(45) Lawrence, M. G.; Jockel, P.; von Kuhlmann, R. *Atmos. Chem. Phys. Discuss.* **2001**, *1*, 43.

(46) Jockel, P.; Brenninkmeijer, C. A. M.; Crutzen, P. J. *Atmos. Chem. Phys. Discuss.* **2002**, *4*, 1261.
(47) Lovelock, J. E. *Nature* **1977**, *267*, 32.
(48) Makide, Y.; Rowland, F. S. *Proc. Natl. Acad. Sci. U.S.A.* **1981**, *78*, 5933.
(49) (a) Prinn, R.; Cunnold, D.; Simmonds, P.; Alyea, F.; Boldi, R.; Crawford, A.; Fraser, P.; Gutzler, D.; Hartley, D.; Rosen, R.; Rasmussen, R. *J. Geophys. Res.* **1992**, *97*, 2445. (b) Prinn, R. G.; Weiss, R. F.; Miller, B. R.; Huang, J.; Alyea, F. N.; Cunnold, D. M.; Fraser, P. J.; Hartley, D. E.; Simmonds, P. G. *Science* **1995**, *269*, 187. (c) Prinn, R. G.; Huang, J.; Weiss, R. F.; Cunnold, D. M.; Fraser, P. J.; Simmonds, P. G.; McCulloch, A.; Harth, C.; Salameh, P.; O'Doherty, S.; Wang, R. H. J.; Porter, L.; Miller, B. R. *Science* **2001**, *292*, 1882.
(50) Krol, M.; van Leeuwen, P. J.; Lelieveld, J. *J. Geophys. Res.* **1998**, *103*, 10697.
(51) Montzka, S. A.; Spivakovsky, C. M.; Butler, J. H.; Elkins, J. W.; Lock, L. T.; Mondeel, D. J. *Science* **2000**, *288*, 500.
(52) Miller, B. R.; Huang, J.; Weiss, R. F.; Prinn, R. G.; Fraser, P. F. *J. Geophys. Res.* **1998**, *103*, 13237.
(53) Volz, A.; Ehhalt, D. H.; Derwent, R. G. *J. Geophys. Res.* **1981**, *86*, 5163.
(54) Mak, J. E.; Southon, J. R. *Geophys. Res. Lett.* **1998**, *25*, 2801.
(55) Quay, P.; King, S.; White, D.; Brockington, M.; Plotkin, B.; Gammon, R.; Gerst, S.; Stutsman, J. *J. Geophys. Res.* **2000**, *105*, 15147.
(56) Prinn, R. G.; Weiss, R. F.; Fraser, P. J.; Simmonds, P. G.; Cunnold, D. M.; Alyea, F. N.; O'Doherty, S.; Salameh, P.; Miller, B. R.; Huang, J.; Wang, R. H. J.; Hartley, D. E.; Harth, C.; Steele, L. P.; Sturrock, G.; Midgley, P. M.; McCulloch, A. *J. Geophys. Res. D* **2000**, *105*, 17751−17792.
(57) Sander, S. P.; Friedl, R. R.; Golden, D. M.; Huie, R. E.; Kurylo, M. J.; Orkin, V. L.; Ravishankara, A. R.; Kolb, C. E.; Molina, M. J.; Finlayson-Pitts, B. J.; Moortgat, G. K. *Chemical Kinetics and Photochemical Data for Use in Atmospheric Studies, Evaluation No. 14*; JPL Publication 02-25; Jet Propulsion Laboratory, California Institute of Technology: Pasadena, CA, 2003.
(58) Prinn, R. G.; Weiss, R. F. Private communication.
(59) Huand, J.; Prinn, R. G. *J. Geophys. Res.* **2002**, *107* (D24), Article No. 4784.
(60) Bridgeman, C. H.; Pyle, J. A.; Shallcross, D. E. *J. Geophys. Res.* **2000**, *105*, 26493.
(61) Wuebbles, D. J.; Patten, K. O.; Johnson, M. T.; Kotamarthi, R. *J. Geophys. Res.* **2001**, *106*, 14551.
(62) Orkin, V. L.; Huie, R. E.; Kurylo, M. J. *J. Phys. Chem.* **1996**, *100*, 8907.
(63) Kaye, J. A.; Penkett, S. A.; Ormond, F. M. *NASA Ref. Pub. 1339*, **1994**.
(64) *Atmospheric Ozone 1985*; Report No. 16; Global Ozone Research and Monitoring Project, World Meteorological Organization: Geneva, Vol. II, 1985.
(65) *U. S. Standard Atmosphere*;U.S. Governent Printing Office: Washington, DC, 1976.
(66) Prather, M. J.; Watson, R. T. *Nature* **1990**, *344*, 729.
(67) Pyle, J. A.; Solomon, S.; Wuebbles, D.; Zvenigorodsky, S. Ozone Depletion and Chlorine Loading Potentials. *Scientific Assessment of Ozone Depletion: 1991*; Report No. 25; Global Ozone Research and Monitoring Project; World Meteorological Organization: Geneva, 1992.
(68) Wuebbles, D. J. *J. Geophys. Res.* **1983**, *88*, 1433.
(69) Solomon, S.; Wuebbles, D. Ozone Depletion Potentials, Global Warming Potentials, and Future Chlorine/Bromine Loading. *Scientific Assessment of Ozone Depletion: 1994*; Report No. 37; Global Ozone Research and Monitoring Project; World Meteorological Organization: Geneva, 1995.
(70) Madronich, S.; Velders, G. J. M. Halocarbon Scenarios for the Future Ozone Layer and Related Consequences; *Scientific Assessment of Ozone Depletion: 1998*; Report No. 44; Global Ozone Research and Monitoring Project; World Meteorological Organization: Geneva, 1999.
(71) Solomon, S.; Mills, M.; Heidt, L. E.; Pollock, W. H.; Tuck, A. F. *J. Geophys. Res.* **1992**, *97*, 825.
(72) Solomon, S.; Albritton, D. L. *Nature* **1992**, *357*, 33.
(73) Daniel, J. S.; Solomon, S.; Albritton, D. L. *J. Geophys. Res.* **1995**, *100*, 1271.
(74) *Climate Change 1990: The Intergovernmental Panel on Climate Change Scientific Assessment*; Cambridge University Press: New York, 1990.
(75) Granier, C.; Shine, K. P. Climate Effects of Ozone and Halocarbon Changes; *Scientific Assessment of Ozone Depletion: 1998*; Report No. 44; Global Ozone Research and Monitoring Project; World Meteorological Organization: Geneva, 1999.
(76) Fisher, D. A.; Hales, C. H.; Wang, W.-C.; Ko, M. K. W.; Sze, N. D. *Nature* **1990**, *344*, 513.
(77) (a) Roehl, C. M.; Boglu, D.; Brühl, C.; Moortgat, G. K. *Geophys. Res. Lett.* **1995**, *22*, 815. (b) Wallington, T. J.; Schneider, W. F.; Sehested, J.; Bilde, M.; Platz, J.; Nielson, O. J.; Christensen, L. K.; Molina, M. J.; Wooldridge, P. W. *J. Phys. Chem. A* **1997**, *101*, 8264.
(78) Orkin, V. L.; Guschin, A. G.; Larin, I. K.; Huie, R. E.; Kurylo, M. J. *J. Photochem. Photobiol., A* **2003**, *157*, 211.
(79) Howard, C. J. *J. Phys. Chem.* **1979**, *83*, 3.
(80) Michael, J. V.; Lee, J. H. *J. Phys. Chem.* **1979**, *83*, 10.
(81) Kaufman, F. *J. Phys. Chem.* **1984**, *88*, 4909.
(82) Atkinson, R. *Chem. Rev.* **1986**, *86*, 69.
(83) Finlayson-Pitts, B. J. *Atmospheric Chemistry*; John Willey & Sons: New York, 1986.
(84) Morris, E. D., Jr.; Niki, H. *J. Chem. Phys.* **1971**, *55*, 1991.
(85) Morris, E. D., Jr.; Niki, H. *J. Phys. Chem.* **1971**, *75*, 3640.
(86) Avramenko, L. I.; Lorenzo, R. V. *Dokl. Akad. Nauk SSSR* **1949**, *67*, 867.
(87) Kaufman, F.; Del Greco, F. P. *Discuss. Faraday Soc.* **1962**, *33*, 126.
(88) Abbatt, J. P.; Demerjian, K. L.; Anderson, J. G. *J. Phys. Chem.* **1990**, *94*, 4566.
(89) Westenberg, A. A.; DeHaas, N. *J. Chem. Phys.* **1965**, *43*, 1550.
(90) Dixon-Lewis, G.; Wilson, W. E.; Westenberg, A. A. *J. Chem. Phys.* **1966**, *44*, 2877.
(91) Takacs, G. A.; Glass, G. P. *J. Phys. Chem.* **1973**, *77*, 1060.
(92) Bradley, J. N.; Hack, W.; Hoyermann, K.; Wagner, H. Gg. *J. Chem. Soc., Faraday Trans. 1* **1973**, *69*, 1889.
(93) Poulet, G.; Jourdain, J. L.; Lavedet, G.; Le Bras, G. *Chem. Phys. Lett.* **1981**, *81*, 573.
(94) Orkin, V. L.; Khamaganov, V. G. *J. Atmos. Chem.* **1993**, *16*, 157.
(95) Howard, C. J.; Evenson, K. M. *J. Chem. Phys.* **1974**, *61*, 1943.
(96) Oehlers, C.; Temps, F.; Wagner, H. Gg.; Wolf, M. *Ber. Bunsen-Ges. Phys. Chem.* **1992**, *96*, 171.
(97) Orkin, V. L.; Khamaganov, V. G. *J. Atmos. Chem.* **1993**, *16*, 157.
(98) Langhaar, H. L. *Am. Soc. Mech. Eng. Trans.* **1942**, *64*, A55.
(99) Kaufman, F. *Prog. React. Kinet.* **1961**, *1*, 1.
(100) Walker, R. E. *Phys. Fluids* **1961**, *4*, 1211.
(101) Poirier, R. V.; Carr, R. W. *J. Phys. Chem.* **1971**, *75*, 1593.
(102) Brown, R. L. *J. Res. Natl. Bur. Stand. (U.S.)* **1978**, *83*, 1.
(103) Gershenzon, Yu. M.; Rozenshtein, V. B.; Spasskii, A. I.; Kogan, A. M. *Dokl. Akad. Nauk SSSR* **1972**, *205*, 624.
(104) Gershenzon, Yu. M.; Rozenshtein, V. B.; Spasskii, A. I.; Kogan, A. M. *Dokl. Akad. Nauk SSSR* **1972**, *205*, 871.
(105) Orkin, V. L.; Khamaganov, V. G.; Larin, I. K. *Int. J. Chem. Kinet.* **1993**, *25*, 67.
(106) Brown, A. C.; Canosa-Mas, C. E.; Parr, A. D.; Wayne, R. P. *Atmos. Environ., Part A* **1990**, *24*, 2499.
(107) Wayne, R. P.; Canosa-Mas, C. E.; Heard, A. C.; Parr, A. D. *Atmos. Environ., Part A* **1992**, *26*, 2371.
(108) Keyser, L. F. *J. Phys. Chem.* **1984**, *88*, 4750.
(109) Loewenstein, L. M.; Anderson, J. G. *J. Phys. Chem.* **1985**, *89*, 5371.
(110) Westbrook, C. K.; Creighton, J.; Lund, C.; Dryer, F. L. *J. Phys. Chem.* **1977**, *81*, 2542.
(111) Seeley, J. V.; Jayne, J. T.; Molina, M. J. *Int. J. Chem. Kinet.* **1993**, *25*, 571.
(112) Abbatt, J. P. D.; Demerjian, K. L.; Anderson, J. G. *J. Phys. Chem.* **1990**, *94*, 4566.
(113) Abbatt, J. P. D.; Fenter, F. F.; Anderson, J. G. *J. Phys. Chem.* **1992**, *96*, 1780.
(114) Clarke, J. S.; Kroll, J. H.; Donahue, N. M.; Anderson, J. G. *J. Phys. Chem. A* **1998**, *102*, 9847.
(115) Donahue, N. M.; Clarke, J. S.; Demerjian, K. L.; Anderson, J. G. *J. Phys. Chem.* **1996**, *100*, 5821.
(116) Donahue, N. M.; Dubey, M. K.; Mohrschladt, R.; Demerjian, K. L.; Anderson, J. G. *J. Geophys. Res.* **1997**, *102*, 6159.
(117) Seeley, J. V.; Jayne, J. T.; Molina, M. J. *J. Phys. Chem.* **1996**, *100*, 4019.
(118) Seeley, J. V.; Meads, R. F.; Elrod, M. J.; Molina, M. J. *J. Phys. Chem.* **1996**, *100*, 4026−4031.
(119) Herndon, S. C.; Villalta, P. W.; Nelson, D. D.; Jayne, J. T.; Zahniser, M. S. *J. Phys. Chem. A* **2001**, *105*, 1583.
(120) Schlicting, H. *Boundary-Layer Theory*; McGraw-Hill: New York, 1979.
(121) Massman, W. J. *J. Geophys. Res.* **1991**, *96*, 15269.
(122) Norrish, R. G. W.; Porter, G. *Nature* **1949**, *164*, 658.
(123) Husain, D.; Norrish, R. G. W. *Proc. R. Soc. London, Ser. A* **1963**, *273*, 165.
(124) Greiner, N. R. *J. Phys. Chem.* **1966**, *45*, 99.
(125) Morley, C.; Smith, I. W. M. *J. Chem. Soc., Faraday Trans. 2* **1972**, *68*, 1016.
(126) Stuhl, F.; Niki, H. *J. Chem. Phys.* **1972**, *57*, 3671.
(127) Stuhl, F.; Niki, H. *J. Chem. Phys.* **1972**, *57*, 3677.
(128) Kurylo, M. J. *Chem. Phys. Lett.* **1973**, *23*, 467.
(129) Davis, D. D.; Fischer, S.; Schiff, R. *J. Chem. Phys.* **1974**, *61*, 2213.
(130) Perry, R. A.; Atkinson, R.; Pitts, J. N., Jr. *J. Chem. Phys.* **1976**, *64*, 1618.
(131) Robertshaw, J. S.; Smith, I. W. M. *J. Phys. Chem.* **1982**, *86*, 785.
(132) Tully, F. P. *Chem. Phys. Lett.* **1983**, *96*, 148.
(133) Forster, R.; Frost, M.; Fulle, D.; Hamann, H. F.; Hippler, H.; Schlepegrell, A.; Troe, J. *J. Chem. Phys.* **1995**, *103*, 2949.
(134) Tully, F. P.; Droege, A. T.; Koszykowski, M. L.; Melius, C. F. *J. Chem. Phys.* **1986**, *90*, 691.

(135) Ravishankara, A. R.; Nicovich, J. M.; Thompson, R. L.; Tully, F. P. *J. Chem. Phys.* **1981**, *85*, 2498.
(136) Hynes, A. J.; Wine, P. H.; Semmes, D. H. *J. Phys. Chem.* **1986**, *90*, 4148.
(137) Davis, D. D.; Heaps, W.; McGee, T. *Geophys. Res. Lett.* **1976**, *3*, 331.
(138) Davis, D. D.; Heaps, W. S.; Philen, D.; Rodgers, M.; McGee, T.; Nelson, A.; Moriarty, A. J. *Rev. Sci. Instrum.* **1979**, *50*, 1505.
(139) Wahner, A.; Ravishankara, A. R. *J. Geophys. Res. D* **1987**, *92*, 2189.
(140) Luque, J.; Crosley, D. R. *J. Chem. Phys.* **1998**, *109*, 439.
(141) Crowley, J. N.; Carl, S. A. *J. Phys. Chem. A* **1997**, *101*, 4178.
(142) Gilles, M. K.; Talukdar, R. K.; Ravishankara, A. R. *J. Phys. Chem. A.* **2000**, *104*, 8945.
(143) Carl, S. A.; Crowley, J. N. *Atmos. Chem. Phys.* **2001**, *1*, 1.
(144) Crank, J. *The Mathematics of Diffusion*; Clarendon Press: Oxford, 1956.
(145) Carslaw, H. S. *Introduction to the Mathematical Theory of the Conduction of Heat in Solids*; MacMillan and Co., Ltd.: London, 1921.
(146) Tully, F. P.; Golgsmith, J. E. M. *Chem. Phys. Lett.* **1985**, *116*, 345.
(147) Orkin, V. L.; Huie, R. E.; Kurylo, M. J. *J. Phys. Chem.* **1996**, *100*, 8907.
(148) Mallard, W. G.; Westley, F.; Herron, J. T.; Hampson, R. F.; Frizzel, D. H. *NIST Chemical Kinetics Database, Version 6.0*; National Institue of Standards and Technology: Gaithersburg, MD, updated 1997.
(149) Atkinson, R.; Carter, W. P. L.; Winer, A. M.; Pitts, J. N., Jr. An Experimental Protocol for the Determination of OH Radical Rate Constants with Organics Using Methyl Nitrite Photolysis as an OH Radical Source. *J. Air Pollut. Control Assoc.* **1981**, *31*, 1090.
(150) Brauers, T.; Finlayson-Pitts, B. J. Analysis of Relative Rate Measurements. *Int. J. Chem. Kinet.* **1997**, *29*, 665.
(151) Atkinson, R.; Aschmann, S. M.; Carter, W. P. L.; Winer, A. M.; Pitts, J. N., Jr. *Int. J. Chem. Kinet.* **1982**, *14*, 781.
(152) Atkinson, R.; Aschmann, S. M.; Pitts, J. N., Jr. *Environ. Sci. Technol.* **1984**, *18*, 110.
(153) Tuazon, E. C.; Carter, W. P. L.; Atkinson, R.; Winer, A. M.; Pitts, J. N., Jr. *Environ. Sci. Technol.* **1984**, *18*, 49.
(154) Atkinson, R.; Winer, A. M.; Pitts, J. N., Jr. *Atmos. Environ.* **1982**, *16*, 1017.
(155) Nielsen, O. J.; Sidebottom, H. W.; O'Farrell, D. J.; Donlon, M.; Treacy, J. *Chem. Phys. Lett.* **1988**, *146*, 197.
(156) Wallington, T. J.; Andino, J. M.; Skewes, L. M.; Siegl, W. O.; Japar, S. M. *Int. J. Chem. Kinet.* **1989**, *21*, 993.
(157) Doyle, G. J.; Lloyd, A. C.; Darnall, K. R.; Winer, A. M.; Pitts, J. N., Jr. *Environ. Sci. Technol.* **1975**, *9*, 237.
(158) Wallington, T. J.; Hurley, M. D. *Environ. Sci. Technol.* **1993**, *27*, 1448.
(159) Orlando, J. J.; Tyndall, G. S.; Wallington, T. J.; Dill, M. *Int. J. Chem. Kinet.* **1996**, *28*, 433.
(160) Goto, M.; Inoue, Y.; Kawasaki, M.; Guschin, A. G.; Molina, L. T.; Molina, M. J.; Wallington, T. J.; Hurley, M. D. *Environ. Sci. Technol.* **2002**, *36*, 2395.
(161) Chen, L.; Kutsuna, S.; Nohara, K.; Takeuchi, K.; Ibusuki, T. *J. Phys. Chem. A* **2001**, *105*, 10854.
(162) Chen, L.; Kutsuna, S.; Tokuhashi, K.; Sekiya, A. *Int. J. Chem. Kinet.* **2003**, *35*, 317.
(163) Ohta, T. *J. Phys. Chem.* **1983**, *87*, 1209.
(164) DeMore, W. B. *Geophys. Res. Lett.* **1992**, *19*, 1367.
(165) DeMore, W. B.; Wilson, E. W., Jr. *J. Phys. Chem. A* **1999**, *103*, 573.
(166) DeMore, W. B.; Bayes, K. D. *J. Phys. Chem. A* **1999**, *103*, 2649.
(167) Chen, L.; Kutsuna, S.; Tokuhashi, K.; Sekiya, A.; Takeuchi, K.; Ibusuki, T. *Int. J. Chem. Kinet.* **2003**, *35*, 239.
(168) Hsu, K.-J.; DeMore, W. B. *J. Phys. Chem.* **1995**, *99*, 1235.
(169) Hsu, K.-J.; DeMore, W. B. *J. Phys. Chem.* **1995**, *99*, 11141.
(170) Campbell, I. M.; Handy, B. J.; Kirby, R. M. *J. Chem. Soc., Faraday Trans. 1* **1975**, *71*, 867.
(171) Barnes, I.; Bastian, V.; Becker, K. H.; Fink, E. H.; Zabel, F. *Atmos. Environ.* **1982**, *16*, 545.
(172) Tuazon, E. C.; Carter, W. P. L.; Atkinson, R.; Pitts, J. N., Jr. *Int. J. Chem. Kinet.* **1983**, *15*, 619.
(173) Finlayson-Pitts, B. J.; Hernandez, S. K.; Berko, H. N. A New Dark Source of the Gaseous Hydroxyl Radical for Relative Rate Measurements. *J. Phys. Chem.* **1993**, *97*, 1172.
(174) Deters, R.; Otting, M.; Wagner, H. Gg.; Temps, F.; Laszlo, B.; Dobe, S.; Berces, T. *Ber. Bunsen-Ges. Phys. Chem.* **1998**, *102*, 58.
(175) Orkin, V. L.; Khamaganov, V. G.; Guschin, A. G.; Huie, R. E.; Kurylo, M. J. *J. Phys. Chem.* **1997**, *101*, 174.
(176) Villenave, E.; Orkin, V. L.; Huie, R. E.; Kurylo, M. J. *J. Phys. Chem.* **1997**, *101*, 8513.
(177) Garland, N. L.; Medhurst, L. J.; Nelson, H. H. *J. Geophys. Res. D* **1993**, *98*, 23107.
(178) *Scientific Assessment of Stratospheric Ozone: 1989*; Report No. 20; Global Ozone Research and Monitoring Project; World Meteorological Organization: Geneva, 1989; Vol. 2, Appendix: AFEAS Report.
(179) Zhang, Z.; Liu, R.; Huie, R. E.; Kurylo, M. J. *J. Phys. Chem.* **1991**, *95*, 194.
(180) Talukdar, R. K.; Mellouki, A.; Gierczak, T.; Burkholder, J. B.; McKeen, S. A.; Ravishankara, A. R. *J. Phys. Chem.* **1991**, *95*, 5815.
(181) Grosjean, D.; Williams, E. L., II. *Atmos. Environ., Part A* **1992**, *26*, 1395.
(182) Orkin, V. L.; Huie, R. E.; Kurylo, M. J. *J. Phys. Chem.* **1997**, *101*, 9118.
(183) Watson, R. T.; Ravishankara, A. R.; Machado, G.; Wagner, S.; Davis, D. D. *Int. J. Chem. Kinet.* **1979**, *11*, 187.
(184) Kozlov, S. N.; Orkin, V. L.; Huie, R. E.; Kurylo, M. J. *J. Phys. Chem.* **2003**, *107*, 1333.
(185) Kozlov, S. N.; Orkin, V. L.; Kurylo, M. J. *J. Phys. Chem.* **2003**, *107*, 2239.
(186) Cvetanovic, R. J.; Overend, R. P.; Paraskevopoulos, G. *Int. J. Chem. Kinet., Symp. 1* **1975**, 249.
(187) Cvetanovic, R. J.; Singleton, D. L. *Int. J. Chem. Kinet.* **1977**, *9*, 481.
(188) Cvetanovic, R. J.; Singleton, D. L. *Int. J. Chem. Kinet.* **1977**, *9*, 1007.
(189) Cvetanovic, R. J.; Singleton, D. L.; Paraskevopoulos, G. *J. Phys. Chem.* **1979**, *83*, 50.
(190) Fontijn, A.; Felder, W. *J. Phys. Chem.* **1979**, *83*, 24.
(191) Heberger, K.; Kemeny, S.; Vidoczy, T. *Int. J. Chem. Kinet.* **1987**, *19*, 171.
(192) Vaghjiani, G. L.; Ravishankara, A. R. *Nature (London)* **1991**, *350*, 406.
(193) DeMore, W. B.; Sander, S. P.; Golden, D. M.; Hampson, R. F.; Kurylo, M. J.; Howard, C. J.; Ravishankara, A. R.; Kolb, C. E.; Molina, M. J. *Chemical Kinetics and Photochemical Data for Use in Stratospheric Modeling, Evaluation No. 12*; JPL Publication 97-4; Jet Propulsion Laboratory, California Institute of Technology: Pasadena, CA, 1997.
(194) Orkin, V. L.; Poskrebyshev, G. A.; Huie, R. E.; Kurylo, M. J. To be submitted for publication.
(195) Singleton, D. L.; Paraskevopoulos, G.; Irwin, R. S. *J. Am. Chem. Soc.* **1989**, *111*, 5248.
(196) Wallington, T. J.; Dagaut, P.; Liu, R. H.; Kurylo, M. J. *Int. J. Chem. Kinet.* **1988**, *20*, 177.
(197) Bilde, M.; Mogelberg, T. E.; Sehested, J.; Nielsen, O. J.; Wallington, T. J.; Hurley, M. D.; Japar, S. M.; Dill, M.; Orkin, V. L.; Buckley, T. J.; Huie, R. E.; Kurylo, M. J. *J. Phys. Chem. A* **1997**, *101*, 3514.
(198) Wollenhaupt, M.; Carl, S. A.; Horowitz, A.; Crowley, J. N. *J. Phys. Chem. A* **2000**, *104*, 2695.
(199) Wallington, T. J.; Ninomiya, Y.; Mashino, M.; Kawasaki, M.; Orkin, V. L.; Huie, R. E.; Kurylo, M. J. J. *J. Phys. Chem. A* **2001**, *105*, 7225.
(200) Smith, I. W. M.; Ravishankara, A. R. *J. Phys. Chem. A* **2002**, *106*, 4798.
(201) Gierczak, T.; Talukdar, R.; Vaghjiani, G. L.; Lovejoy, E. R.; Ravishankara, A. R. *J. Geophys. Res.* **1991**, *96*, 5001.
(202) Kwok, E. S. C.; Atkinson, R. *Atmos. Environ.* **1995**, *29*, 1685.
(203) Atkinson, R. *Chem. Rev.* **1986**, *86*, 69.
(204) Atkinson, R. *Int. J. Chem. Kinet.* **1987**, *19*, 799.
(205) Atkinson, R. *Environ. Toxicol. Chem.* **1988**, *7*, 435.
(206) DeMore, W. B. *J. Phys. Chem.* **1996**, *100*, 5813.
(207) Louis, F.; Gonzalez, C. A.; Huie, R. E.; Kurylo, M. J. *J. Phys. Chem.* **2000**, *104*, 2931.
(208) Louis, F.; Gonzalez, C. A.; Huie, R. E.; Kurylo, M. J. *J. Phys. Chem.* **2000**, *104*, 8773.
(209) Louis, F.; Gonzalez, C. A.; Huie, R. E.; Kurylo, M. J. *J. Phys. Chem.* **2001**, *105*, 1599.

CR020524C